A Comprehensive Study of Poly(2,3,5,6-tetrafluoroaniline): From Electrosynthesis to Heterojunctions and Ammonia Sensing

Mickaël Mateos, Rita Meunier-Prest, Olivier Heintz, Frédéric Herbst, Jean-Moïse Suisse, Marcel Bouvet

Graphical Abstract

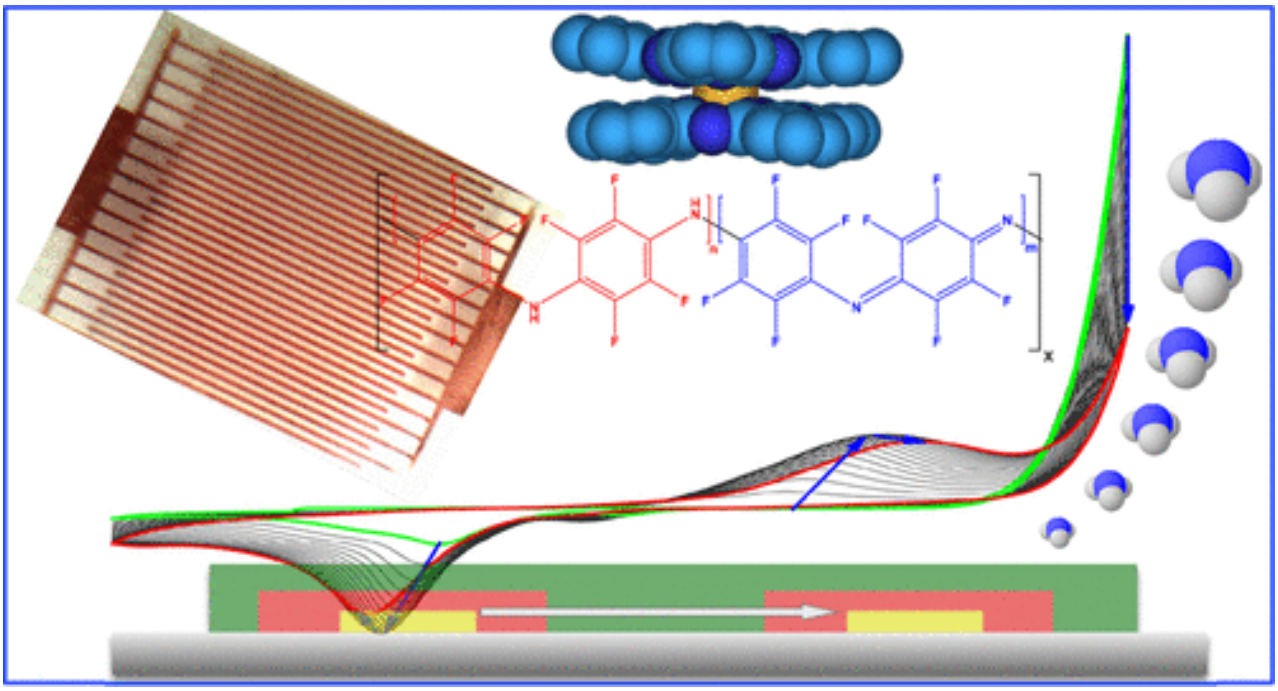

A comprehensive study of poly(2,3,5,6-tetrafluoroaniline): from electrosynthesis to heterojunctions and ammonia sensing

Mickaël Mateos[a], Rita Meunier-Prest[a], Olivier Heintz[b], Frederic Herbst[b], Jean-Moïse Suisse[a], Marcel Bouvet[a]**

[a]Institut de Chimie Moléculaire de l'Université de Bourgogne (ICMUB), UMR CNRS 6302, Université Bourgogne Franche-Comté, 9 avenue Alain Savary, 21078 Dijon cedex, France. Tel: +33-380-396-086; E-mail: marcel.bouvet@u-bourgogne.fr; rita.meunier-prest@u-bourgogne.fr

[b]Laboratoire Interdisciplinaire Carnot de Bourgogne (LICB), UMR CNRS 6303, Université Bourgogne Franche-Comté, 9 avenue Alain Savary, 21078 Dijon cedex, France

Keywords. electrodeposition, conducting polymer, fluorinated material, XPS, electrochemical quartz crystal microbalance, heterojunction, ammonia sensor,

Abstract. In this work, we report for the first time on a comprehensive study of poly(2,3,5,6-tetrafluoroaniline (PTFANI). Contrary to the non fluorinated polyaniline or its analogues bearing one fluorine atom, PTFANI is a poorly conductive material. We present a comprehensive study of the electrosynthesized PTFANI from its monomer in acidic aqueous medium. PTFANI was fully characterized by a potential-pH diagram, spectroelectrochemistry, and electrochemical quartz crystal microbalance (EQCM) measurements, as well as by a morphological study. Combined with XPS analysis, it allowed us to understand the redox properties of this polymer compared to those of the unsubstituted polyaniline. At pH < 1.85, no proton transfer occurred during the electrochemical process, but the insertion of anions at the site of the protonated imines was demonstrated through EQCM and XPS experiments. PTFANI showed a lower ratio of 1 ClO_4^- per 3 TFANI units compared to that of PANI. The behavior at pH > 1.85 was different; no anion upload was observed during the electron transfer, but 1 H^+ per electron was involved during the transition between the leucoemeraldine base and emeraldine base forms. It should also be noted that the oxidation of the emeraldine into pernigraniline form was not accessible in PTFANI, due to the electron-withdrawing effects of fluorine atoms. However, we took advantage of the unique behavior of PTFANI to build heterojunctions, by combination with a highly conductive molecular material, namely lutetium bisphthalocyanine, $LuPc_2$. The obtained double lateral heterojunction exhibited a particularly interesting sensitivity to ammonia, even under humid atmospheres, with a limit of detection of 450 ppb. This work paves the way for the use of PTFANI in other electronic devices and as a sensor not only in the field of air quality monitoring but also in the field of health diagnosis by measurement in human breath.

1. Introduction

Since the discovery of the metallic state of chemically or electrochemically doped polyacetylene $(CH)_x$, conducting polymers have been widely studied,[1] beginning with polyaniline (PANI), polypyrrole (PPy) and polythiophene (PT). Their ease of shaping by solution processing techniques associated with their ability to replicate the electrical properties of ordinary inorganic semiconductors allow for the emergence of organic electronics, with the development of low-cost plastic electronic devices.[2] Since their conducting properties are related to their doping state,[3] conducting polymers are especially suitable for the detection of redox active species in conductometric sensors.[4,5] They were even used as sensing materials to design electronic noses.[6] Electropolymerization is a particularly well suited technique to synthesize conducting polymers, since it allows, in the same step, synthesizing a polymer, shaping a material and controlling its conducting state, and also its electrical, optical properties and its chemosensitivity.[7] As other conducting polymers, polyaniline is currently used as a sensing material in chemical sensors. These sensors are mainly conductometric transducers as resistors[8-11] and field-effect transistors,[7,12] even though other types of transducers are also used.[13]

In the field of electronics, it is known that beside the high performance of silicon integrated circuits, a market exists for lower performing but extremely inexpensive circuits. With this aim, solution processes can advantageously replace the classic vapor deposition technique. The concept of solution processing covers all the topics of organic electronics, from thin film transistors for active-matrix OLED displays to organic photovoltaic cells. The field of chemical sensors that requires low-cost devices to multiply measuring points, e.g. for air quality monitoring, is particularly suitable for molecular materials, especially for polymers. Many solution processes can be applied, such as ink-jet printing, solvent-cast, spin-coating, or even 3D printing. However,

electrodeposition offers net advantages, for example when different materials need to be deposited on the same substrate. Thus, electrochemistry provides unique techniques for specifically addressing an electrode.

The electronic properties of conducting polymers are highly dependent on the nature of the substituents and their physico-chemical properties as well, such as their growth behavior and their solubility. Thus, polyanilines synthesized from aniline bearing electron-donating substituents such as methoxy groups[14,15] and electron-withdrawing substituents such as halogen atoms[16,17] have been reported. Polymerization of fluorine-containing aniline monomers have been performed chemically and electrochemically starting from 2-fluoroaniline, 3-fluoroaniline and 4-fluoroaniline.[18] However, as long as the aniline bears one or two halogen atoms, a conducting state can be obtained via a chemical or electrochemical process. Beyond, for the perfluoroaniline, due to the accumulation of electron-withdrawing effect of four fluorine atoms per aromatic ring, particular electronic transport properties are expected. However, contrary to the unsubstituted polyaniline (PANI), the obtained materials remain not fully characterized, and only two papers deal with the perfluoroaniline.[19,20] The electrochemical oxidation of 2,3,5,6-tetrafluoroaniline (TFANI) was first reported by J. Cassidy, in 1991.[19] He published a new study twenty years later, devoted in particular to the electrochromic properties of the corresponding polymer.[20] The most important reported result is that the polymer film deposited on ITO does not display important color variations, changing from orange to more bleached orange when going from positive to negative applied potential. However, the absorbance variation, associated to a low color efficiency compared to other electrochromic materials, is typically less than a twelfth of the efficiency of PEDOT containing films. Actually, this was observed when the polymer film was immersed in a solution containing the monomer. We can consider that the absorbance

modification of the polymer film is assisted by the monomer. Another possibility is that the increase of the absorbance under oxidation could be due to the generation of additional polymer and the decrease to the instability of the polymer under reduction. The main goal, through several electrochemical characterizations (E-pH diagram, spectroelectrochemistry and EQCM measurements) combined with XPS analysis, is to understand the redox properties of this polymer in comparison with the unsubstituted polyaniline. Finally, we report a new way to prepare organic heterojunctions based on PTFANI and study their sensitivity to ammonia.

2. Experimental section

Chemicals.

2,3,5,6-tetrafluoroaniline (TFANI), 99.7% acetic acid, 85% phosphoric acid, boric acid, 70% perchloric acid, KOH and KCl were purchased from Sigma Aldrich and used as received. $K_3Fe(CN)_6$ and $K_4Fe(CN)_6$ were purchased from Arcos Organics and used as received. Absolute ethanol (analaR normapur) was purchased from Carlo Erba. Aniline (Aldrich) was distilled at 120°C under reduced pressure before use. All perchloric acid solutions were prepared by dilution from 70 % $HClO_4$. Ammonia gas, at 985 ppm and 98 ppm (mol/mol) in synthetic air, and synthetic air were used from standard gas cylinders, purchased from Air Liquide, France. Lutetium bisphthalocyanine ($LuPc_2$) was synthesized according to previously described methods.[21] All Britton-Robinson buffers (pH 1.8 to 8) were prepared according to described methods.[22]

Cleaning procedure of working electrodes.

Carbon disk electrode was soaked for 10 min in 2 M KOH, polished with 0.1 μm alumina, and sonicated for 10 minutes, first in EtOH then in water, and finally rinsed with $HClO_4$. ITO plate

electrodes and ITO interdigitated electrodes (IDE, deposited onto a 1 x 1 cm² floated glass substrate and separated by 75 μm with 50 nm thickness) were sonicated for 10 min in CH_2Cl_2 then in acetone, EtOH and water. Then, the electrodes were dried under air flow and rinsed with 2 M $HClO_4$. Gold grid electrode (80 mesh, BioLogic) for spectroelectrochemical measurements was sonicated for 10 min in EtOH and water, successively.

Electrochemical methods.

All electrochemical experiments were performed with a PGSTAT302 N (Metrohm) potentiostat connected to a PC and the collected data were analyzed using Nova® 2.1 software. Cyclic voltammetry (CV) and chronoamperometry (ChA) were carried out by means of a three-electrode setup consisting of a glassy carbon disk (GC, 3 mm diameter, Bioanalytical Systems) or Indium Tin Oxide (ITO) plate (9 mm diameter of active surface, 8-12 Ω of square resistance, Solems, France) or IDE as working electrode, a platinum wire as counter electrode and a saturated calomel electrode (SCE) isolated from the solution by a 2 M $HClO_4$ salt bridge as reference electrode. Potentials were reported versus SCE. PANI films were deposited on ITO plates by chronoamperometry at 1 V in a solution of 0.15 M aniline in 2 M $HClO_4$ with a surface charge of 265 $mC.cm^{-2}$, then rinsed with 0.1 M $HClO_4$, absolute EtOH and dried under vacuum at room temperature. PTFANI films were prepared on ITO plates and IDE by chronoamperometry at 1.4 V in a 50 mM solution of TFANI in 2 M $HClO_4$. The electrolysis was stopped after consuming 250 $mC.cm^{-2}$. The modified electrode was rinsed in 0.1 M $HClO_4$ and water then dried under vacuum at room temperature.

Electrochemical Quartz Crystal Microbalance.

Electrochemical quartz crystal microbalance (EQCM) measurements were performed with a QCA922A system (Seiko-EG&G, Princeton Applied Research) in a microelectrochemical cell

(Biologic 092-QCA-FC model), equipped with a gold coated quartz crystal (Biologic SE-9C-M, resonance frequency of 9 MHz with an active surface of 0.2 cm^2), a platinum wire as counter electrode and an Ag/AgCl reference electrode. Considering that the deposited layer is rigid (no viscoelastic changes occur at the electrode interface) the relationship between the frequency change and the mass change was calculated from the chronocoulometry of a solution of 5 mM $CuSO_4$ in 1 M H_2SO_4 at -0.4 V *vs* Ag/AgCl (1 Hz = 5.5 $ng.cm^{-2}$). EQCM experiments were carried out to monitor the ion transfer of PTFANI film as a function of pH. First, two films were deposited by chronoamperometry at 1.4 V in a 50 mM solution of TFANI in 2 M $HClO_4$ (surface charge of 33 $mC.cm^{-2}$ with a frequency shift of 2 kHz) and 2 M CH_3COOH (surface charge of 62 $mC.cm^{-2}$ with a frequency shift of 19.83 kHz). Then, a 0.1 M $HClO_4$ solution was introduced into the circulation cell to wash the first film until the pH of the output solution was 1 and a cyclic voltammetry was carried out from - 0.3 V to 1.3 V at 20 $mV.s^{-1}$. The same procedure was then performed with pH 4 acetate buffer on the second film prepared in acetic acid.

UV-visible spectroelectrochemistry.

The film formation and the spectroelectrochemical characterization of the polymer films were carried out using a UV-visible diode array spectrometer (KINSPEC II/MMS-16 VIS, BioLogic). The 150-W Xe lamp and the spectrometer were connected to the quartz glass cell (optical length = 1 mm) by light fibers. The cell was equipped for electrochemical measurements with a gold grid (80 mesh, BioLogic) as working electrode, a platinum wire (0.5 mm diameter) as counter electrode and a SCE as reference. PTFANI was deposited by chronoamperometry at 1.25 V (surface charge of 250 $mC.cm^{-2}$ that corresponds to a theoretical thickness of 1 µm of PTFANI in its intermediate state) in a solution of 50 mM TFANI in $HClO_4$ 2 M.

Electrosynthesis of PTFANI powder.

A 2 M $HClO_4$ solution containing 0.1 M TFANI was electrolyzed 6 times under magnetic stirring and deposited on a platinum basket at a constant current (50 mA). At the end of each electrolysis, the working electrode was rinsed in 0.2 M $HClO_4$ to remove the monomer. The polymer was then dissolved in absolute EtOH. Each electrolysis was stopped when the potential reached 1.6 V. Then, the dissolved polymer was purified by precipitation in EtOH / 0.2 M $HClO_4$.

Chemical and thermal Characterization (IR, NMR, TGA, DSC).

The infrared spectra were recorded on a Bruker Vector 22 with KBr pellet, in transmission mode. NMR spectra were recorded using a BRUKER 300 MHz Avance III Nanobay spectrometer. ^{1}H NMR spectra were calibrated with respect to TMS on the basis of the relative chemical shift of the residual non-deuterated solvent as an internal standard and ^{19}F NMR spectra were calibrated with respect to $CFCl_3$. Melting points (mp) were measured by differential scanning calorimetry (DSC Q1000 V9.9 Build 303). Experiments were performed under nitrogen, at a heating rate of 20 °C.min^{-1}. Thermogravimetric analyses (TGA) were performed on a TA Instruments TGA Q500 thermoanalyzer using platinum pans, under flowing nitrogen gas. Weight loss percentages and onset temperatures were determined using the TA Universal Analysis 2000 software provided with the instrument.

SEM images and XPS analysis.

SEM images were performed with a scanning electronic microscope JEOL JSM6400F with 2 kV of acceleration voltage. XPS analysis of the PTFANI powder and polymer films deposited on ITO was performed on a SIA100 spectrometer (Cameca Riber apparatus) using non-monochromated Al Kα X-ray source (1486.6 eV photons). All spectra were calibrated using the

normalized In($3d_{5/2}$) XPS signal from In_2O_3 at 444.8 eV,[23] and all deconvolutions were performed using contributions with nearly constant FWHM (+/- 0.2 eV).

Electrical and chemosensing measurements.

The top layer was coated over the PTFANI sublayer prepared on IDEs, by sublimation of the bisphthalocyanine of lutetium ($LuPc_2$) in an UNIVEX 250 thermal evaporator (Oerlikon, Germany), under secondary vacuum (ca. 10^{-6} mbar), at a rate of 1 Å.s^{-1}, by heating in a temperature range of 400-500 °C. The apparatus used for NH_3 exposure, at different relative humidity (RH) values, was described previously.[24] The total flow was in the range 0.5-0.55 L.min^{-1} depending on ammonia concentration and the volume of the test chamber was 8 cm^3. Gas sensing experiments were carried out in a dynamic way, by alternating 4 min-long rest periods and 1 min-long exposure periods.

3. Results and Discussion

Monomer oxidation with film formation.

Cyclic voltammetry of TFANI was recorded in aqueous acidic solution using a glassy carbon (GC) electrode (Fig. 1a) or an ITO plate (Fig. 1b). On a GC electrode, the first anodic scan shows an irreversible anodic peak at 1.24 V, then, on the returned sweep, two cathodic peaks at 0.50 V and 0.20 V. On the second scan, a new anodic peak arises at 0.76 V. As the number of scans increases, the cathodic peaks are shifted towards lower values, the anodic peak at 0.76 V is shifted towards higher potentials and the intensity of the anodic peak at 1.24 V decreases. The irreversible anodic peak at 1.24 V corresponds to the oxidation of the monomer (TFANI). Its intensity lowers as the polymer is made. The occurrence of signals in the region 0-1 V is indicative of the formation of the polymer. The shift of the peak potentials and the diminution of

the current intensity with the expansion of deposited material (Fig. 1b) are characteristic of an increasing resistance and of a decreasing conductivity of the polymer. This behavior is consistent with a previous report on the formation of a PTFANI film onto ITO.[20] However, on ITO, the oxidation peak of the monomer is hidden by the anodic limit of the electrochemical window (Fig. 1b); an higher resistance is observed, due to the resistivity of the ITO plates and characterized by a greater separation between cathodic and anodic peaks.

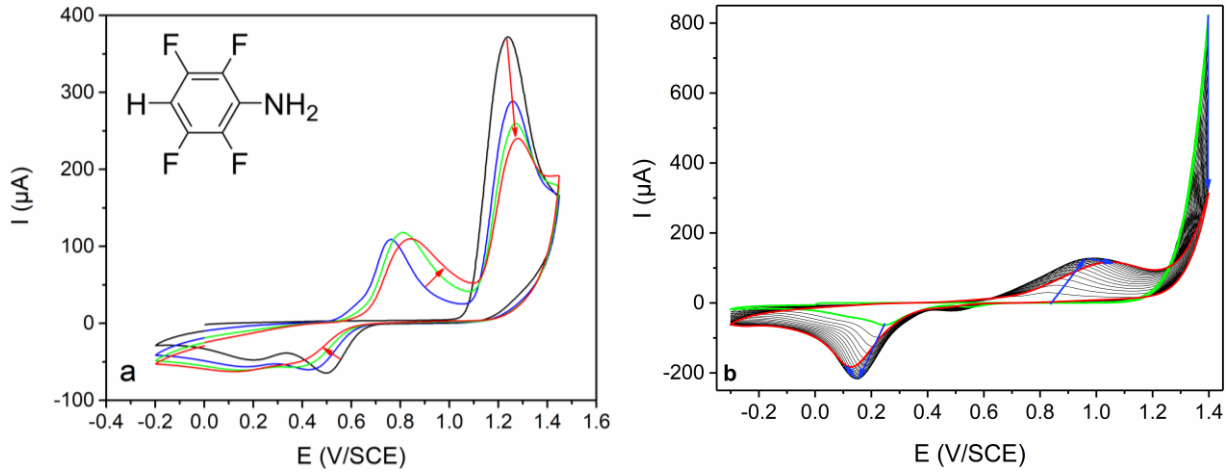

Figure 1. a) Cyclic voltammogram of 30 mM TFANI in 0.7 M $HClO_4$ on a GC disk (3 mm in diameter) at 0.1 $V.s^{-1}$; b) cyclic voltammogram of 50 mM TFANI in 2 M $HClO_4$ on ITO electrode at 0.04 $V.s^{-1}$.

Electrochemical characterization of the film.

PTFANI films were also deposited by electrolysis of the monomer at 1.4 V (250 $mC.cm^{-2}$). The PTFANI chronoamperometric curve has a different shape than the chronoamperometric curve of PANI (Fig. S1). In particular, it does not exhibit a minimum, generally attributed to nucleation processes at the electrode surface. This behavior can be related to a different mechanism of polymerization and especially a different rate limiting-step. The obtained brown film is denser and thicker than the one obtained by cyclic voltammetry. Additional information

on its conductivity is provided by the electrochemical response of a molecular probe at the film-coated electrode. In this study, potassium ferro/ferricyanide was used because it undergoes a reversible, one-electron, outer-sphere redox reaction.[25] Its charge transfer was investigated through the PTFANI film acting as a barrier that can reduce or even block the charge transfer. Two PTFANI-coated electrodes were prepared: the first one was made by cycling the potential 20 times from -0.2 to 1.4 V; the second one by applying a potential of 1.4 V until a charge of 162 mC was consumed, which corresponds to seven times the one that passed during CV deposition. Both modified electrodes were then dipped in a solution of ferro/ferricyanide and their CV responses compared to that of a bare electrode (Fig. 2). It should be noted that, due to the resistivity of the ITO plate, the potential peak difference obtained on the bare electrode is greater than that expected theoretically (120 mV instead of 58 mV). The voltammogram of the ITO electrode modified by a PTFANI film deposited by CV reveals a partial blocking effect of the film resulting in a decrease of the intensity of both anodic and cathodic peaks and an increase of the separation between them. This phenomenon is enhanced on the PTFANI-coated ITO electrode made by chronoamperometry: the response of the couple $Fe(CN)_6^{3-}/Fe(CN)_6^{4-}$ is no longer visible and its charge transfer appears completely blocked. Contrary to PANI, which is a conducting polymer, the presence of fluorine in PTFANI makes the material more insulating. Based on the charge consumed during the deposition process, the thickness of the film can be estimated to be 1 µm by chronoamperometry and 125 nm by CV. The film obtained by application of a constant potential is thicker and constitutes therefore a better barrier to the electron transfer.

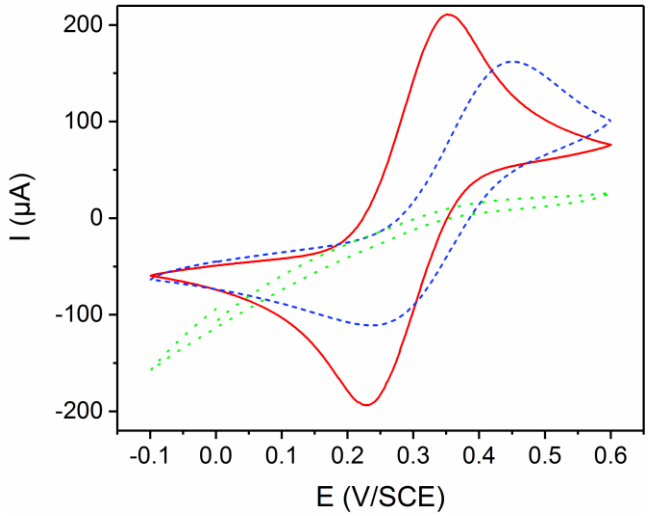

Figure 2. Cyclic voltammogram of 10^{-3} M $K_3[Fe(CN)_6]$ + 10^{-3} M $K_4[Fe(CN)_6]$ in 0.1 M KCl, at 0.1 V s^{-1}, on a bare ITO electrode (red line) and on a PTFANI-coated ITO plate obtained by cyclic voltammetry (blue dashed line) or by chronoamperometry at 1.4 V (green dotted line).

Typical electrochemical responses of PANI or PTFANI films coated ITO electrodes, in monomer-free aqueous $HClO_4$ solution are presented in Fig. 3. The cyclic voltammogram of PANI exhibits, as expected, two redox systems.[26] The first oxidation step, at +0.33 V, corresponds to the transformation of the leucoemeraldine form in the protonated emeraldine form of the polyaniline. The second step, at +0.6 V, is the oxidation of the emeraldine form in pernigraniline form. For PTFANI films, only one anodic peak is observed at 1.4 V, shifted by more than 1 V compared to that of PANI. This peak is followed, on the reverse scan, by a reduction peak of near-equal intensity (I_{pc} / I_{pa} = 0.99). Anodic and cathodic peaks are separated from each other by more than 1.4 V. The current density of the response of PTFANI is very low compared to that of PANI prepared under the same conditions (in both cases a charge of nearly 250 mC cm^{-2} was consumed). Both findings reveal the poor conductivity of PTFANI. The large shift of the redox system is due to the fluorination of the aniline ring, which makes the oxidation more difficult, and also to the low conductivity of the polymer.

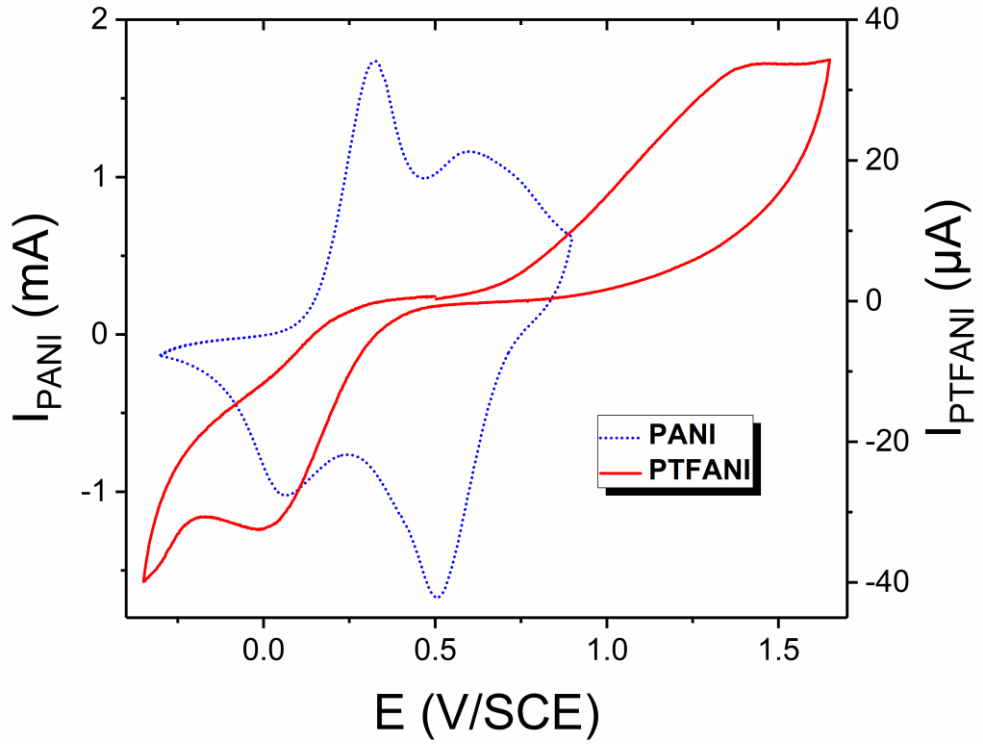

Figure 3. Cyclic voltammograms of ITO electrodes coated with 1 µm PANI (blue dotted line) and PTFANI (red line) films prepared by chronoamperometry respectively at 1 V (charge surface of 265 mC cm^{-2}) or at 1.4 V (charge surface of 250 mC cm^{-2}), in 0.5 M $HClO_4$, at 0.04 $V.s^{-1}$.

In acidic medium, the intensity of the anodic and cathodic peaks of PTFANI are found to vary linearly with the square root of the scan rate as it is for PANI.[27] This behavior can be attributed to the diffusion of ions in the polymer and was previously reported for PTFANI in presence of the monomer.[20] We also studied dimethoxyaniline, which is oxidized at a potential slightly less positive than the aniline, +0.7 V against +0.8 V vs SCE, respectively, whereas TFANI is oxidized more difficultly, at a voltage of 1.4 V vs SCE, all values being determined in the same experimental conditions. We electrosynthesized the poly(2,5-dimethoxyaniline), which is also a highly conducting polymer, since its emeraldine salt is easily obtained,[14] as this of PANI and contrarily to what's happen for PTFANI.

Influence of the pH on the electrochemical behavior of the films.

The cyclic voltammograms of PTFANI were recorded at different pH in order to study the influence of protons. The electrochemical behavior of PTFANI films was compared to that of polyaniline. Assuming that bipolarons are formed, as was proposed by Huang et al.,[26] we chose to give a schematic representation of the redox mechanism involving tetrameric subunits of the polymer (scheme 1). More detailed schemes including the molecular structure of all the forms are given in supporting information (Fig. S2 and Fig. S3). Electrons and protons exchanges corresponding to Laviron's square scheme theory[28-30] appear vertically. The *pKa* of the different forms is associated to horizontal equilibria. This is a simplified view of the process because the studied polymers are polyelectrolytic materials that do not have precise dissociation constants but a distribution of them. However, in a first approximation, this constitutes a useful diagrammatic representation to gain more insight into the mechanism.

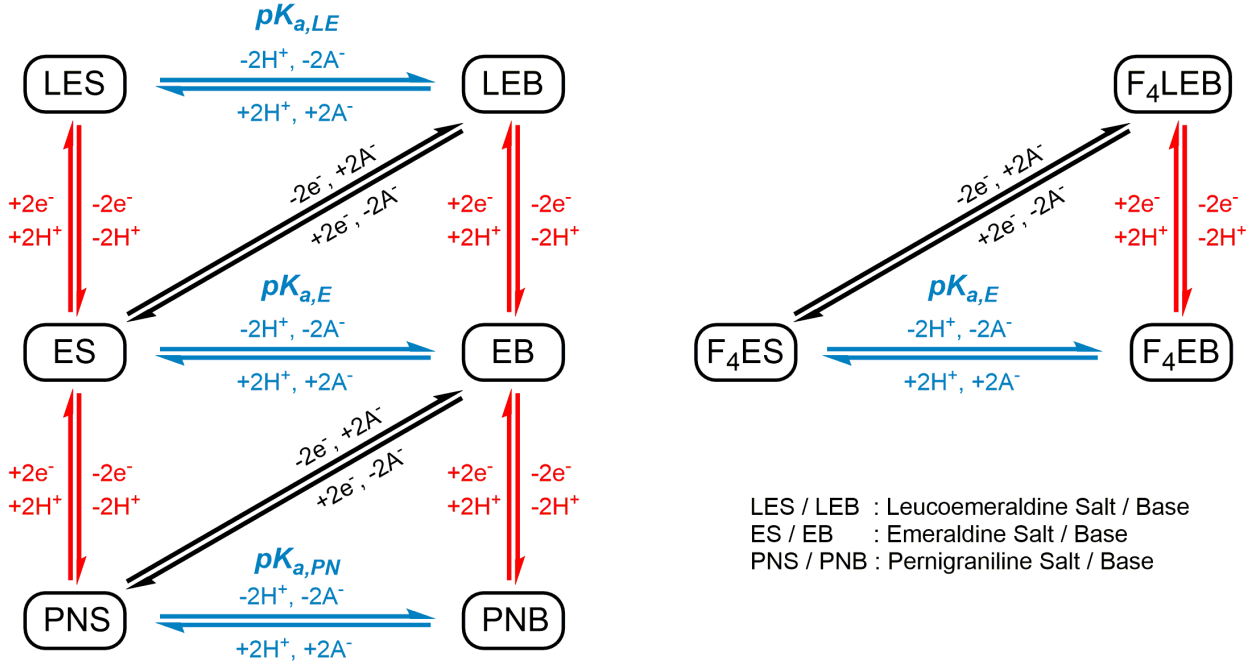

Scheme 1. Reaction scheme for PANI (left) and for PTFANI (right). The indicated number of e^-, H^+ and A^- is for one tetrameric unit. The molecular structures are given in Fig. S2 and Fig. S3.

First of all, we reexamined the literature results for PANI. We reported in Fig. 4, the different values of the half-wave potentials, $E^1_{1/2}$, of the first redox system (leucoemeraldine – emeraldine transformation) and $E^2_{1/2}$, of the second redox system (emeraldine – pernigraniline transformation). They were obtained, at different pH values, either by spectroscopic[31] or electrochemical measurements.[26,27,32] For the highest concentrations, the acidity function H_0 that takes into account the fact that the activity cannot be assimilated to the concentration is used instead of pH.[33] The $E_{1/2}$ – pH or acidity function H_0 diagram contains several zones:

- For acidity function $H_0 < 0.76$, $E^1_{1/2}$ values vary linearly with H_0 with a slope of -66 mV / H_0 units. The leucoemeraldine salt (LES) is oxidized during an electrochemical process involving as much protons as electrons to give the conductive protonated emeraldine salt (ES), in accordance with the corresponding vertical process (LES – ES in scheme 1). The second redox system is found to vary linearly with pH with a slope of -120 mV / pH unit, indicating the involvement of two protons per electron. It corresponds to the transformation of ES in the pernigraniline base (PNB).

- For $0.76 < pH < 3$, the potential of the first system remains invariant with the pH; no proton transfer occurs in the first redox process, as shown in the diagonal equilibrium LEB – ES (scheme 1), whereas two protons per electron are still transferred in the second stage (ES – PNB). The pH value at 0.76 corresponds to the acid-base equilibrium between LES and LEB, i.e. the protonation of the amine according to equation (1):

$$-NH_2^+ \leftrightarrows -NH- + H^+ \quad (K_{a,LE}) \text{ (1)}$$

This is slightly smaller than the value that was reported earlier[34,35] but in the same range than some of the more recent results.[36] Similarly, pH 3 corresponds to the acid-base equilibrium between ES and EB, i.e. the protonation of the imine according to equation (2):

$$= NH^+ \leftrightarrows = NH - + H^+ \quad (K_{a,E}) \quad (2)$$

The literature pK_{aE} values were collected by Marmisollé et al.[37] A great dispersion was observed, which can be attributed to the different conditions of polymer synthesis.

- For 3 < pH < 7, the base forms are the most stable. The potential of both systems varies linearly with the pH, with slopes of respectively -50 and -66 mV / pH unit, showing the implication of one proton per transferred electron. When increasing the potential, LEB is oxidized to EB, which is oxidized to PNB.

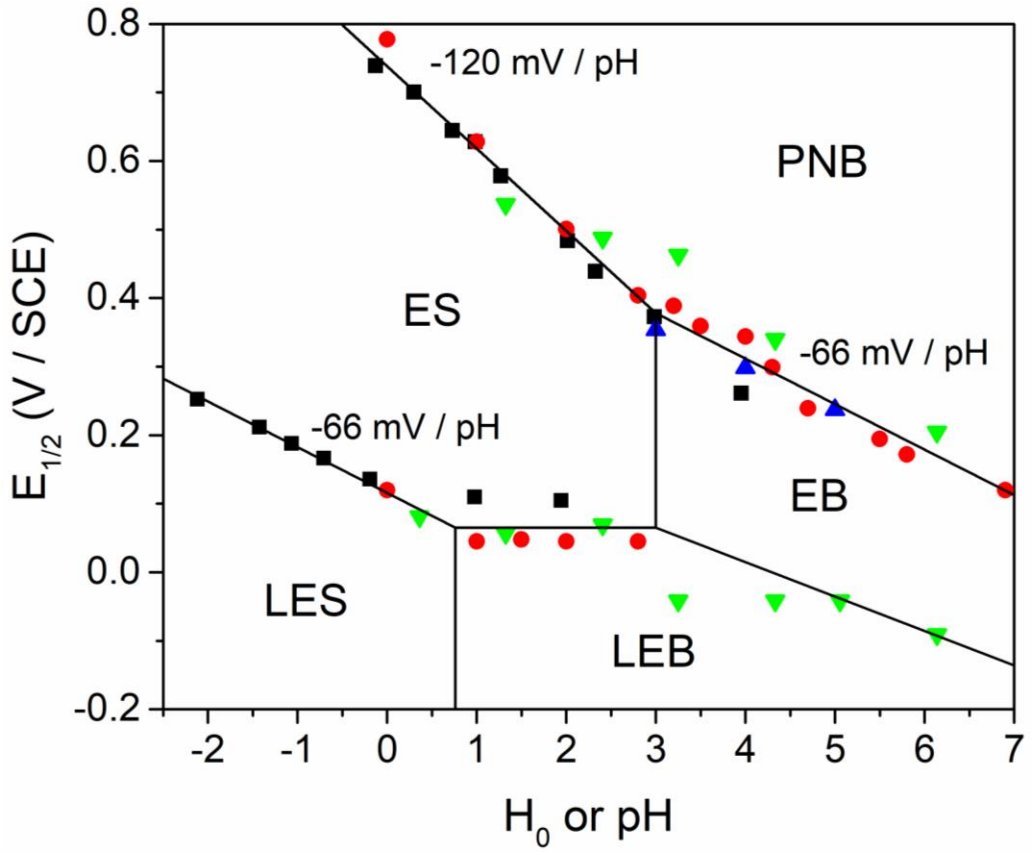

Figure 4. $E_{1/2}$ – pH or acidity function H_0 (see text) diagram of PANI. Variations of the potentials, determined in the literature, for the first ($E^1_{1/2}$) and the second ($E^2_{1/2}$) redox processes, from bottom to top, with the pH : (■) Huang et al. [26]; (●) Focke et al. [27]; (▲) Huang et al. [32]; (▼) Cushman et al.[31]

The $E_{1/2}$ – pH or acidity function H_0 diagram of PTFANI was presented in Fig. 5. We preferred reporting the anodic peak potential, E_{pa}, instead of $E_{1/2}$, because the anodic and cathodic peaks (Fig. 3) were quite distant from each other. In the 1.85 – 7 pH range, the peak potential varies linearly with the pH with a slope of -62 mV / pH unit (Fig. 5) indicating that the same number of protons and electrons is transferred during the electrochemical oxidation of PTFANI (F_4LEB – F_4EB).

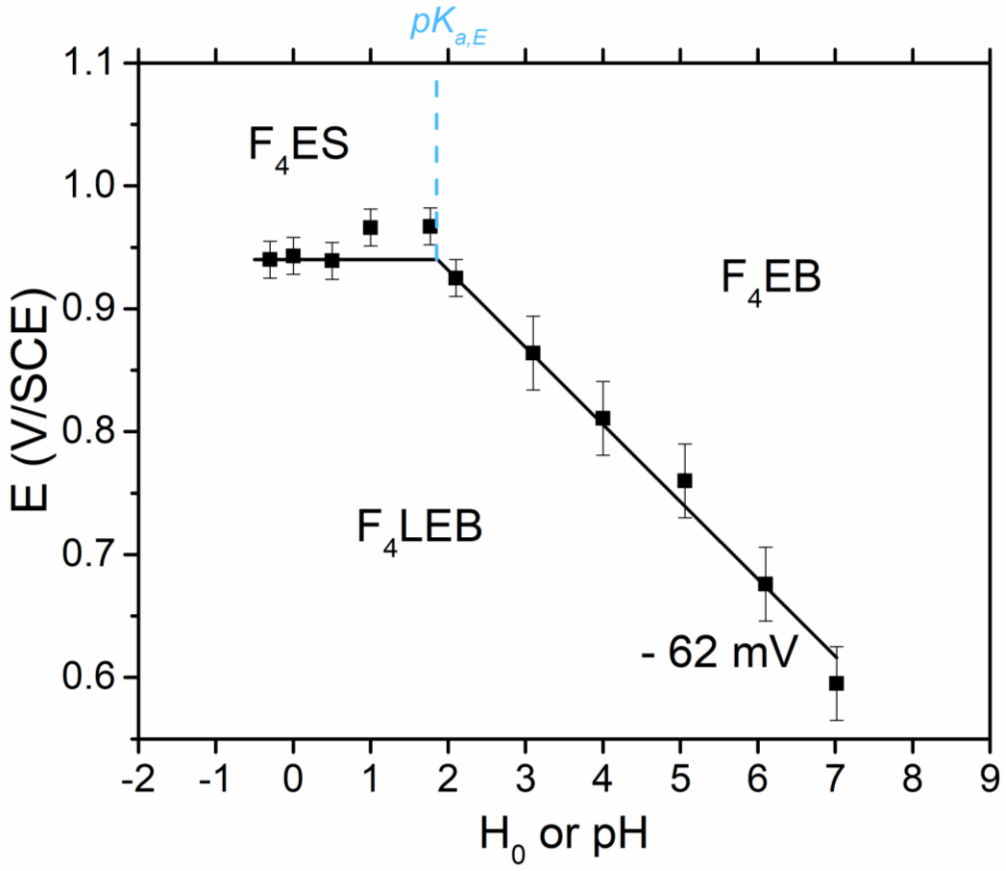

Figure 5. $E_{1/2}$ – pH or acidity function H_0 (see text) diagram of PTFANI. Variations of the potentials, E_{pa}, with the pH.

Below these values, the potential remains invariant with the pH indicating that no proton is involved in the electrochemical process (F_4LEB-F_4ES). In acidic medium, the transition between

the slopes 0 and - 62 mV / pH units corresponds most certainly to the acid-base equilibrium F_4ES-F_4EB characterized by its $pK_{a,E}$. Indeed, this constant can be estimated using the Hammett relation on the basis of the influence of the fluorinated substituents[38] and of the $pK_{a,E}$ value for PANI. The fluorinated groups induced a decrease of the acidic constant by ca. 1.6 pH unit that corresponds roughly to the observed value ($pK_{a,E}$ = 1.85). Compared to PANI, only the first redox system is observed (scheme 1). In summary, the reduced polymer corresponds to the F_4LEB form. At pH above 1.85, its oxidation provides the release of protons to give F_4EB, while F_4ES should be obtained in acidic medium (pH < 1.85). The oxidation mechanism should involve insertion of anions but no more proton exchange.

EQCM measurements.

In order to confirm the different forms involved in the equilibrium diagram of PTFANI (Fig. 5), the ions exchange during the leucoemeraldine - emeraldine transition was investigated at two different pH, one lower (pH 1) and the other higher (pH 4) than the slope change corresponding to the acidic constant, $pK_{a,E}$. First, the gravimetric monitoring of the *in-situ* deposition of PTFANI on the Au coated resonator was performed by chronoamperometry at 1.4 V either in perchloric or in acetic acid. The choice of the acid was driven by the need for a solution with a pH close to that used in the ion transport analysis experiment. Actually, the polymer adheres weakly to gold, so, when the deposition pH is significantly lower than the one of the analysis solution, high quantities of solvent are required to wash the polymer, which results in its peeling.

- pH 1: The deposition of PTFANI was performed in a 2 M $HClO_4$ solution. The formation of the film was confirmed by a mass increase. The experiment was stopped after consumption of 6.6 mC and a shift in frequencies of $\Delta f(PTFANI)$ = - 2000 Hz. If the deposition process is the

same as the one of PANI, i.e. if it involves 2.7 electrons per molecule of monomer, the thickness of the film can be estimated to 0.12 µm. A 0.1 M $HClO_4$ solution was introduced into the circulation cell. The polymer was washed until the pH of the output solution was equal to 1. Cyclic voltammograms were then recorded together with the difference in quartz frequency (Fig. 6). On the forward scan, a mass increase was detected during the anodic process corresponding to a mean shift in frequencies of $\Delta f(ClO_4^-)$ = - 300 Hz. Conversely, on the reverse scan, the frequency raised by approximately the same mean value of $\Delta f(ClO_4^-)$ = + 275 Hz. On oxidation, ClO_4^- anions are inserted into the polymer in order to compensate the positive charge formed, while on reduction, they are expelled, in agreement with the diffusion of ions observed during the cyclic voltammetry in acidic medium (the peak potential varies with $v^{1/2}$). The ratio of the number of ClO_4^- anions per TFANI unit, was calculated from equation (3):

$$(ClO_4^-/TFANI) = \frac{\Delta f(ClO_4^-)}{M_{ClO_4^-}} \times \frac{M_{TFANI}}{(\Delta f(PTFANI) - \Delta f(ClO_4^-))} \quad (3)$$

with M_{ClO4-} and M_{TFANI} being the molecular weight of ClO_4^- and TFANI, respectively.

During the anodic scan, (0.29 ± 0.04) perchlorate anion per TFANI unit are introduced into the polymer, whereas during the cathodic scan (0.26 ± 0.04) perchlorate anion per TFANI unit are ejected.

Thus, in the pH region where no proton is involved during the electrochemical process (pH < 1.85), the gravimetric monitoring confirms the exchange of perchlorate anions and confirms that the oxidized form is the F_4ES form, doped with 1 ClO_4^- anion per 3 TFANI units (Fig. S3).

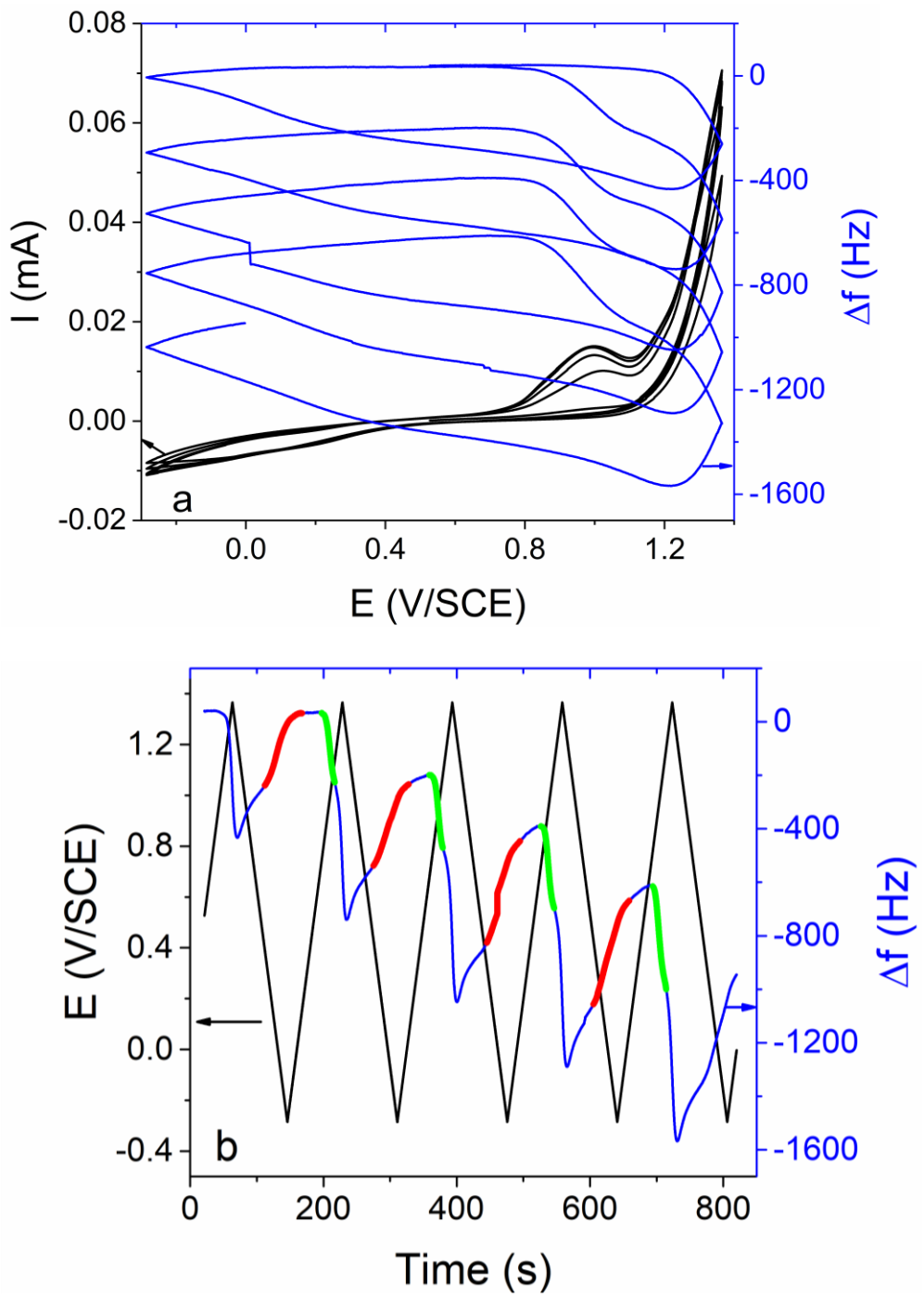

Figure 6. a) Cyclic voltammogram and concomitant in situ monitoring of the frequency variations measured by EQCM on PTFANI coated Au-quartz resonator in 0.1 M $HClO_4$; b) variations of the potential and of the difference in frequency with time during the same experiment as a. The mass uptake is marked in green and the mass release in red.

- pH 4: The polymer was electrochemically prepared in the same way as previously, except that the deposition solvent was a 2 M CH_3CO_2H solution. A rapid mass increase was observed inducing a drop of the frequency $\Delta f(PTFANI)$ = - 19830 Hz. The film was washed by flowing a solution (pH 4) of CH_3CO_2H + 0.1 M CH_3CO_2K into the cell until the pH of the output solution was 4. The cyclic voltammetry presents both anodic and cathodic peaks shifted toward lower potentials compared to those at pH 1, in agreement with the $E_{1/2}$ – pH or acidity function H_0 diagram. The gravimetric monitoring in the course of the cyclic voltammograms reveals a very low mass fall located at the cathodic peak potential. The frequency difference decreased as the number of cycles increased, respectively $\Delta f(CH_3COO^-)$ = 78 Hz for the first, 65 Hz for the second and 50 Hz for the third cycles. The proportion of acetate anions exchanged during the electrochemical study is calculated from equation (1) by replacing ClO_4^- by CH_3COO^-. The mean ratio is $(CH_3COO^- / TFANI)$ = 0.009. At this pH, a very low quantity of anion (0.9 %) is released from the polymer. This process is accelerated by the uptake of protons during the reduction, but it is not correlated to the redox mechanism because no acetate anions are picked up on the reverse anodic scan. It is a "passive" release of CH_3COO^- anions from the polymer. It can be concluded that, in this pH range (from pH 1.85 to pH 7) no anion is involved during the F_4LEB - F_4EB transition. This corroborates the assumption that the transition affects the leucoemeraldine and the emeraldine polymers in their base forms and involves the exchange of one proton per electron but no anion.

Spectroelectrochemistry of a PTFANI film.

The in-situ UV-visible spectra were recorded during the electrochemical deposition of the PTFANI film, at 1.4 V, on a gold grid, in an acidic solution (2 M $HClO_4$ or CH_3COOH). In 2 M

$HClO_4$, the monomer spectrum shows one band at 264 nm. During the electrolysis, a bathochromic shift of the band was observed (λ = 286 nm) and new bands grew: two small bands at 330 and 555 nm and a larger one at 445 nm. Then, the monitoring of the UV-visible spectra was recorded at a fixed potential in the electrodeposition solution. At the anodic peak potential of PTFANI, the absorbance spectrum remains the same attesting that the polymer electrodeposited at 1.4 V is in its oxidized form. On the contrary, when a potential of -0.2 V was set, evolution of the spectra was observed (Fig. 7). The band at 445 nm declined rapidly while the band at 286 nm increased slightly. When the electrolysis was forced for a long time, the intensity of the band at 286 nm dropped as a result of the destruction of the polymer (872 s in Fig. 7).

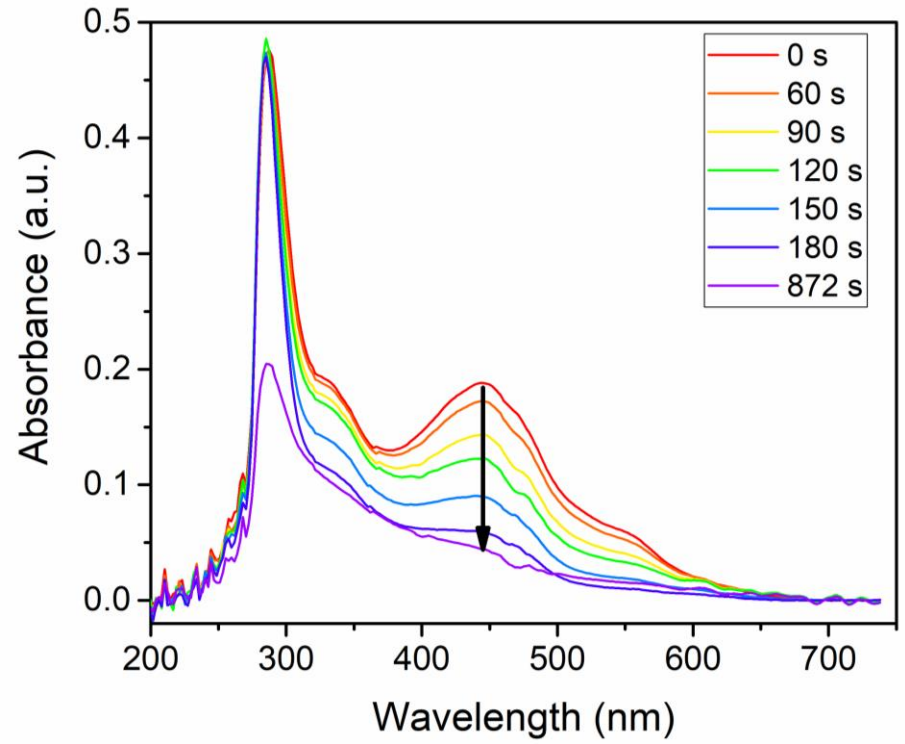

Figure 7. Monitoring of the absorbance spectra of an ITO electrode coated with a PTFANI film, in 2 M $HClO_4$, + 50 mM TFANI, when a reduction potential of - 0.2 V / SCE was imposed.

This is the first report on the monitoring of the electronic absorption spectra of PTFANI over a broad range of wavelength (200-720 nm) at different imposed potentials. Astratine et al.[20] have already presented this kind of study but over a small wavelength range (420-720 nm) and they obtained a very low potential effect characterized by an absorbance variation of less than 0.03 a.u., possibly due to a rather thin polymer film. Moreover, it should be noted that the reversibility of the absorbance that they observed when switching the applied potential from 0 to 1.2 V was assisted by the presence of monomer in the solution.

In the literature, few other studies were devoted to the mono-fluorinated polymers.[18,39-41] Compared to the behavior of PANI, the introduction of a fluorinated group in the aromatic ring of aniline produces a blue shift.[18,39-41] The electronic spectra of the different forms of the polyaniline were already reported.[42,43] The reduced form, LEB, presents only one band at 320 nm, whereas the intermediate form, EB, has two bands at 320 and 640 nm, and the oxidized form, PNB, shows 3 bands at 280, 320 and 530 nm. Each of the conversions LEB - EB and EB - PNB occurs in a one redox step with no intermediate oxidation state.[42] In the case of PTFANI, the electrodeposited film is in the emeraldine form. Its UV-visible spectrum presents two main absorptions at 286 and 445 nm (t = 0 in Fig. 7) that are shifted in the blue region compared to the bands of PANI. This hypsochromic shift is more important than the one observed with the monofluorinated polymer (296 and 496 nm).[18] This is consistent with PTFANI being less basic than PANI due to the substitution of electron withdrawing groups on the polymer backbone. On the contrary, electron-donating substituents, such as methoxy groups induced a red shift. For example, the band at 320 nm for PANI is located at 375 nm for poly(2,5-dimethoxyaniline).[44] Thus, it can be suggested that the band at 286 nm is associated with the $\pi-\pi^*$ transition on the benzene ring and that the band at 445 nm is associated with the $\pi-\pi^*$ transition on the quinoid

ring. The oxidation state of PTFANI can be roughly estimated by the ratio of the intensity of both bands. It is approximately one quinoid per 2 benzenoid rings (Fig. S3). This result is consistent with the ratio ClO_4^- / TFANI unit obtained by EQCM (eq. 3). As the F_4EB is reduced in F_4LEB, the band at 445 nm tends to disappear, due to the reduction of the quinoid ring. At the end of the reduction, only the band at 286 nm corresponding to the $\pi-\pi*$ transition on the benzenoid ring remains visible.

Chemical and thermal characterizations (IR, NMR, TGA, DSC).

The FT-IR spectrum of PTFANI powder (Fig. S4) showed a broad peak at 1610-1640 cm^{-1} attributed to C=C of the quinoid ring and a huge one at 1508 cm^{-1} associated with C=C of benzenoid ring.[45] The high intensity of the band at 1508 cm^{-1} demonstrated the predominance of the benzenoid form. However, because of the broad signal of the quinoid ring, the oxidation degree of the polymer could not be determined. Other relevant peaks at 1378, 1282 and 1180 cm^{-1} were respectively attributed to C-N-C stretching quinoid and benzenoid sequence[45] and finally C-F bonds.[46]

DSC thermogram of PTFANI powder at 20 °C.min^{-1} (Fig. S5) showed a broad endothermic transition, from -10 °C to 60 °C, attributed to the fusion of TFANI (mp = 32 °C) and short PTFANI oligomers. A second one, from 70 °C to 100 °C (maximum at 89 °C), was attributed to the fusion of PTFANI polymer.

The TGA analysis (Fig. S6) from 25°C to 300 °C at 10 °C.min^{-1} under nitrogen showed a weight loss from 105 °C assigned to removal of H_2O, a decomposition temperature (defined as > 10% weight loss) at 170 °C and finally a weight loss of 45% at 300 °C. The thermal stability of the PTFANI is lower than that of the polymonofluoroanilines, which had a decomposition

temperature around 300 °C.[45] PTFANI was analyzed by ^{1}H and ^{19}F NMR spectroscopies in deuterated acetone and its spectra were interpreted taking account the spectra of the monomer (TFANI, Fig. S7, Fig. S8). J_{F-F} couplings on a benzene ring are well known. J_{F-F} ortho is close to 20 Hz whereas J_{F-F} varies in a broad range for meta (-20 Hz to +20 Hz) and for para (+ 5 Hz to +20 Hz) positions. For PTFANI, only the terminal H and amines are expected in the ^{1}H NMR spectrum of PTFANI. Several triplets of triplets (tt) are visible on the spectrum (Fig. S9). The more intense appears at 7.85 ppm, shifted by more than 1.2 ppm compared to TFANI, due to the condensation of the amine with another fluorinated aromatic ring. The coupling constants, $J_{H\text{-}F2,F3}$ = 10.0 Hz and $J_{H\text{-}F1,F4}$ = 7.5 Hz are close to those measured on the TFANI spectrum. The 1H NMR spectrum of PTFANI showed traces of unreacted TFANI (tt at 6.59 ppm), and another triplet of triplet centered at 7.00 ppm, which can be attributed to the dimer. Furthermore, two broad singlets of equal integration at 8.33 and 9.89 ppm suggest the existence of two types of amines.[47] Non resolved multiplets between 7.0 and 7.7 ppm could be attributed to oligomers. From the integration values, we can say that for 100 polymer chains, 18 dimers and 9 monomeric molecules are still present. Since we only see the terminal 1H, the weight ratio is much more favorable to the polymeric form. The ^{19}F NMR spectrum (Fig. S10) shows two main peaks of equal intensities, at -151.75 ppm and -140.31 ppm that can be attributed to two different chemical environments for F atoms, as already reported for poly(3-fluoroaniline).[18] Indeed, it is important to point out that for a uniform polymeric chain, e.g. F_4LEB, all the F atoms should be chemically equivalent, except those from terminal units.

SEM images and XPS analysis.

SEM images emphasized the different morphology of the PTFANI and PANI films, both electroplated on ITO substrates by ChA (Fig. 8). The center of the PTFANI film had a very compact structure that completely covered the substrate and included amorphous grains of polymer of few µm in size. At the edges, the film had a lower thickness and a heterogeneous morphology like oil puddles that did not cover the surface properly. This results from the slow growth of the PTFANI on the surface (strong decrease of the current during the ChA) because this fluorinated polymer has a weak affinity for ITO and a low conductivity that passivates the substrate. Thus, in order to achieve a homogeneous coverage of the substrate, we consumed an important charge. On the contrary, the high conductivity of the PANI film in its ES form allowed a rapid growth on itself (cf section Electrochemical characterization of the film[48]) leading to the formation of fibers of a few hundred nanometers in length that completely covered the substrate (Fig. 8c).

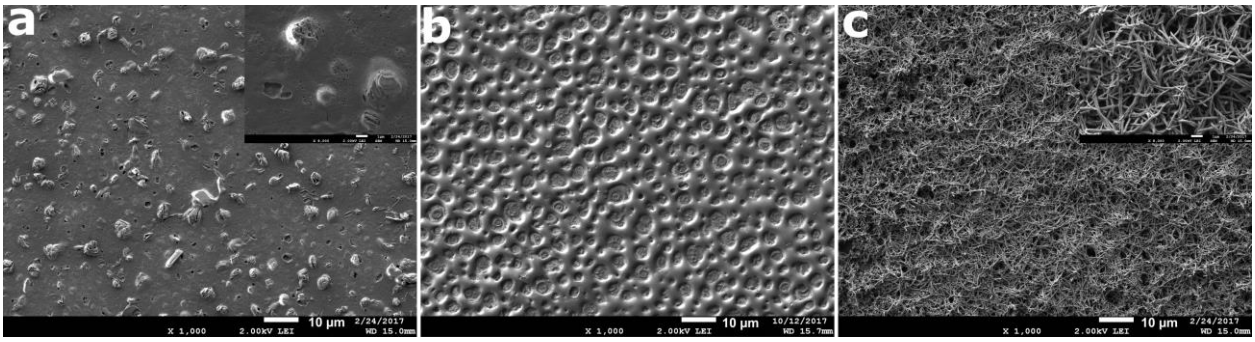

Figure 8. SEM images on ITO substrate of: a) PTFANI film with a zoom (x8) in insert, b) PTFANI at the border of the film, c) PANI film with a zoom (x8) in insert.

The atomic ratio (N(1s) used as reference) has been calculated using peak areas of C(1s), N(1s), O(1s), F(1s) and Cl(2p) for PTFANI and PANI films coated on ITO substrate (Table 1). The results for PANI were in very good agreement with the expected values (5.7 vs 6 expected

for C/N ratio). The important presence of chlorine atoms and the expected O/Cl ratio demonstrates the presence of ClO_4^- counterions that indicates an important acid-base doping (protonation of amine/imine bridges). The large C/N and O/Cl ratios for PTFANI indicate a carbon and oxygen pollution at the surface. The F/N ratio of 3.7 was in good agreement with the expected one (4). The low Cl/N ratio (0.3) for PTFANI compared with PANI (0.8) indicates a lower acid-base doping. However, it was not simple to compare these results because the PANI film was rinsed with EtOH contrary to the PTFANI film, which was quickly rinsed with water because it is soluble in polar organic solvents.

	C(1s) / N(1s)	O(1s) / N(1s)	F(1s) / N(1s)	Cl(3p) / N(1s)	O(1s) / Cl(3p)
PTFANI	7.3 (6)	1.4	3.7 (4)	0.3	5.3 (4)
PANI	5.7 (6)	3.1		0.8	4 (4)

Table 1. XPS results: measured atomic ratio and theoretical values (in brackets) of the PTFANI and PANI films

The C1s spectrum of PTFANI film (Fig. 9) decomposed in four components: 284.9 eV (C-N), 286.6 eV (C-F [49]), 288.9 eV (maybe C=O from polymer degradation) and 292.6 eV (satellite peak from π-π* transition[50]). For PANI, the C1s spectrum showed three components at 284.1 eV (aromatic carbon, expected at 284.5 eV [50]), 285.4 eV (C-N [51]) and 287.1 eV (maybe C-O from polymer degradation[52]).

The O(1s) and Cl(2p3/2) (Fig. S11) spectra for PANI and PTFANI films showed respectively a peak at 531.8 eV and 207 eV that matched with perchlorate ion.[53,54] The F(1s) spectrum of PTFANI film (Fig. S12) showed a peak at 686.8 eV that can be attributed to semi-ionic C-F.[41]

The deconvolution of PANI N1s spectrum (Fig. 9) revealed three different components at 399.3 eV, which represented 48% of the N1s total area, attributed to neutral amine, 401.5 eV (45%) and 403.4 eV (7%) that can be attributed to the protonated imine and the last one to the protonated amine, respectively.[41,53] Nevertheless, the protonated nitrogen contribution (52%) did not match the high chlorine ratio (0.8), suggesting a lack of rinsing. For PTFANI film, the N(1s) spectrum decomposed into three contributions at 399.1 eV (70% of the total area) attributed to neutral amine, 401.1 eV (26% of the area) attributed to protonated imine and 403.8 eV (3% of the area) attributed to protonated amine. The protonated nitrogen contributions (29%) perfectly matched the value of Cl/N ratio (0.3). Despite XPS gives only information on the upper surface of the polymer, this ratio is the same obtained by EQCM measurements (one perchlorate per 3 monomer units), which is a technique that quantify anion insertion through the entire thickness of the polymer layer (1 μm). These observations allowed us to conclude that PANI and PTFANI were both in the emeraldine salt form, with a ratio -N= / -NH- ≈ 1 and 0.4, respectively. This lower value for PTFANI is due to the presence of fluorine atoms on the aromatic ring that makes difficult the oxidation of the polymer and the protonation of the imine moieties.

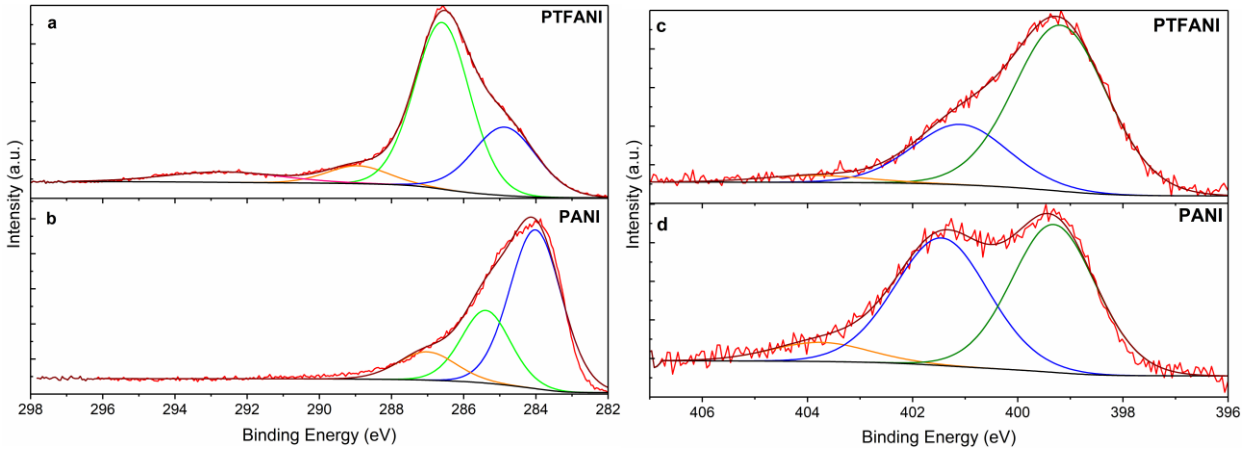

Figure 9. XPS high resolution spectra of a) PTFANI C(1s), b) PANI C(1s), c) PTFANI N(1s), d) PANI N(1s).

Electrical and sensing properties.

First, resistors were prepared by solvent cast from electrosynthesized PTFANI powder (100 µL of EtOH solution at 4 $mg.mL^{-1}$), deposited dropwise on IDE. The substrates were heated at 40 °C in a closed desiccator to facilitate the solvent evaporation and increase the homogeneity of the films and finally dried under vacuum to fully remove the solvent. The I(V) characteristics in the range of ±10 V in ambient atmosphere revealed that these devices were too resistive to precisely determine the conductivity of the polymer. Taking into account the IDE geometry and the detection limit of our electrometer (10 pA at 1 V), we only can deduce an upper limit value of 2.10^{-9} $S.cm^{-1}$ for PTFANI, which is a conductivity lower than that of PANI, even in its EB form.[53] Contrary to most conducting polymers used as sensing materials in chemoresistors,[4,55,56] the conductivity of PTFANI is too low for its use in such a device. So, inspired by the behavior of Molecular Semiconductor-Doped Insulator heterojunction (MSDI) (Scheme 2), patented by one of the authors,[57] we decided to incorporate this insulating material into heterojunctions. MSDIs devices combine two molecular materials, a poorly conducting material deposited on interdigitated electrodes and a highly conductive upper layer of lutetium bisphthalocyanine, $LuPc_2$, which is an intrinsic semiconductor.[58] Depending on the nature of the majority charge carriers in the sublayer, an energy barrier between the two layers arises, which governs the electronic behavior of the device. The key point is that, to circulate through the device, charges have to cross the interface between the two layers. Also, MSDIs are neither diodes nor transistors. MSDIs were prepared with pentacene, oligothiophene and metallophthalocyanines as p-type sublayers, and with perylene derivatives, perfluorometallophthalocyanines[57] and recently with a triphenodioxazine derivative[59] as n-type sublayers.

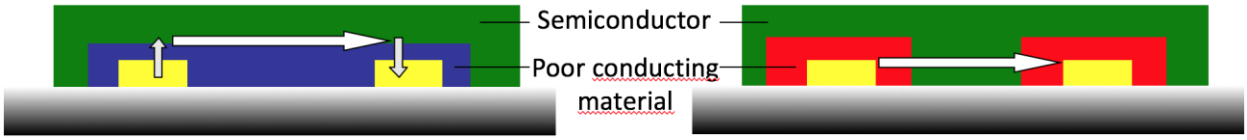

Scheme 2. Schematic views of a MSDI heterojunction (left) and of a double lateral heterojunction (right); the arrows indicate the main channel for charge carriers.

Thus, a PTFANI film of 1 µm thickness was electroplated on IDE and a $LuPc_2$ upper layer was then deposited by evaporation under secondary vacuum, leading to double lateral heterojunction, as shown in the right part of scheme 2. In this new device, mobile charges have to cross twice the interface between the poor conducting material and the $LuPc_2$ semiconducting top layer, as in MSDIs. As observed for abovementioned MSDI heterojunctions,[60] the I-V characteristic of this device showed a non-linear behavior comparing to the ohmic characteristics of a $LuPc_2$ resistor (Fig. 10a). However, the electrochemical deposition process of the insulating layer allowed us to access a new lateral configuration of MSDI heterojunction. Therefore, free charge carriers are forced to cross in a row two ITO / PTFANI interfaces and twice the PTFANI / $LuPc_2$ heterojunction, which created an energy barrier that explained the non-linear behavior at low bias of this device.

Under exposition to NH_3, in dry air and at a 50 % relative humidity (RH), this double lateral heterojunction showed a current drop (Fig. 10b), as expected for a p-type MSDI.[57] Thus, we demonstrated that in in such a PTFANI/$LuPc_2$ heterojunction, the properties are governed by positive charge carriers. The full fluorination of the material does not change the nature of the majority charge carriers, that remains identical in PTFANI and PANI, contrary to what generally happens when molecular materials, e.g. phthalocyanines[61] and pentacene,[62] are fluorinated. Indeed, the metallic regime of polyaniline requires the protonation of neutral imine from

emeraldine base form to reach a poly(semiquinone radical cation) resonance form that has a polaronic conduction band.[53] The withdrawing effect of fluorine atoms of the aniline ring limits the formation of protonated imine and the radical resonance form. This explains the poor conductivity of PTFANI. However, the fluorination cannot reverse the charge carrier creation to obtain a n-type material as observed for oligothiophene derivatives.[63]

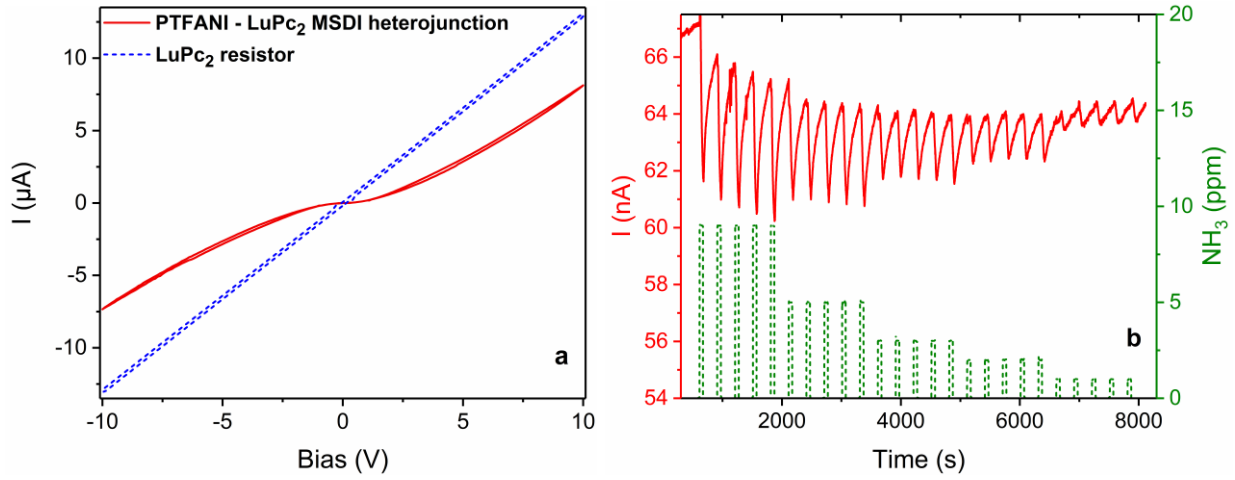

Figure 10. (a) I(V) characteristics in ambient atmosphere of a PTFANI/$LuPc_2$ heterojunction (red solid line) and $LuPc_2$ resistor (blue dashed line), (b) current response of a PTFANI/$LuPc_2$ heterojunction exposed to NH_3 (9, 5, 3, 2 and 1 ppm), in air at 50 % RH, during exposure / recovery cycles (1 min / 4 min).

Since the only material in contact with the atmosphere is the $LuPc_2$ top layer, the first effect of ammonia is to neutralize the majority charge carriers (positive) by an electron transfer from NH_3 molecules towards $LuPc_2$ molecules leading to a higher resistance of the $LuPc_2$ layer, as reported for $LuPc_2$ resistors.[60] Additionally, this decrease of the density of majority charge carriers could also modify the charge transport at the interface between PTFANI and $LuPc_2$.

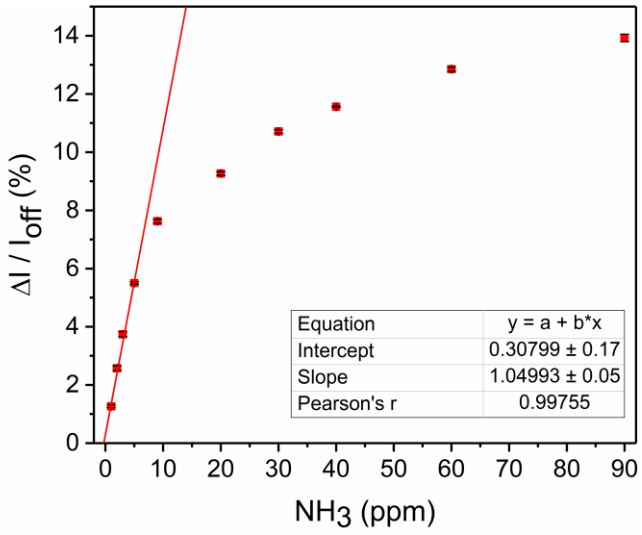

Figure 11. Relative response of a PTFANI/$LuPc_2$ heterojunction as a function of the NH_3 concentration in the 1-90 ppm range, in air at 50 % RH, during exposure / recovery cycles (1 min / 4 min). The data of the linear fit are given in insert.

The study in the 1-90 ppm range (Fig. 10b and Fig. S13) shows that the decrease in current varies with the NH_3 concentration, but not linearly in the full range (Fig. 11). Thus, the relative response (RR) defined as $RR = \Delta I/I_{off} = |I_{on}-I_{off}|/I_{off}$, where I_{on} and I_{off} are the current values at the end and at the beginning of exposure periods, respectively, shows two behaviors. At concentrations higher than 10 ppm, RR is ca. 9.3±0.1% at 20 ppm NH_3 (mean value with standard deviation from all exposition cycles at this concentration), 11.6±0.02% at 40 ppm and 13.9±0.1% at 90 ppm. At concentrations lower than 10 ppm, RR varies linearly with the NH_3 concentration, with a Pearson's r = 0.998. The sensitivity S, defined as the slope of the linear regression of the RR as a function of the NH_3 concentration, is 1.05% ppm^{-1}. These values demonstrate that this device is more suitable for the detection of NH_3 at low concentrations. We determined the limit of detection (LOD) from equation 4:

$$LOD = 3\ N / (S \times I_{off}) \qquad (4)$$

where N is the noise, determined at 1 ppm on the curve I(t) (Fig. 10b).

With N being 0.1 nA and I_{off} 64 nA, a LOD of 450 ppb was deduced. It is important to remember that the daily exposure limit in Europe for NH_3 is 20 ppm, as defined by the European air quality labor legislation[64]. Many detectors that cover this range are available for sale. However, their main default is their sensitivity to humidity variations, which is an issue since NH_3 needs to be detected in industrial environments where the humidity levels can vary in a broad range.[13] More interesting, with this sub-ppm LOD, the present sensor could be used in the field of health diagnosis by measurement in human breath.[65]

Ammonia sensing under humid atmosphere (Fig. 12) was then carried out in the 10-70% range of RH. The response during NH_3 exposition still showed a current drop. This sensor recovers quickly its baseline current, which remains stable over expositions at a given RH value. The I_{off} current decreases when the relative humidity increases, from 174 nA (mean value over 4 cycles) at 10% RH up to 118 nA at 70 % RH, as expected for a p-type device. Indeed, the non-binding oxygen doublets in H_2O neutralize holes in $LuPc_2$, which are the majority charge carriers, leading to a current decrease under humidity. The higher baseline current compared to this observed at a constant RH value (Fig. 10b) can be explained by the duration of the periods in dry air. After a long stay in air at a constant RH, the baseline was kept (Fig. S10). However, the current variation during the exposure period does not depend strongly on the RH value. At 30 ppm, the current variation ΔI during the 1 min exposure phase is in the range of 14.8 to 16.6 nA, at 60 ppm between 17.8 and 19.6 nA and at 90 ppm between 21.1 and 22.5 nA (Fig. 12b).

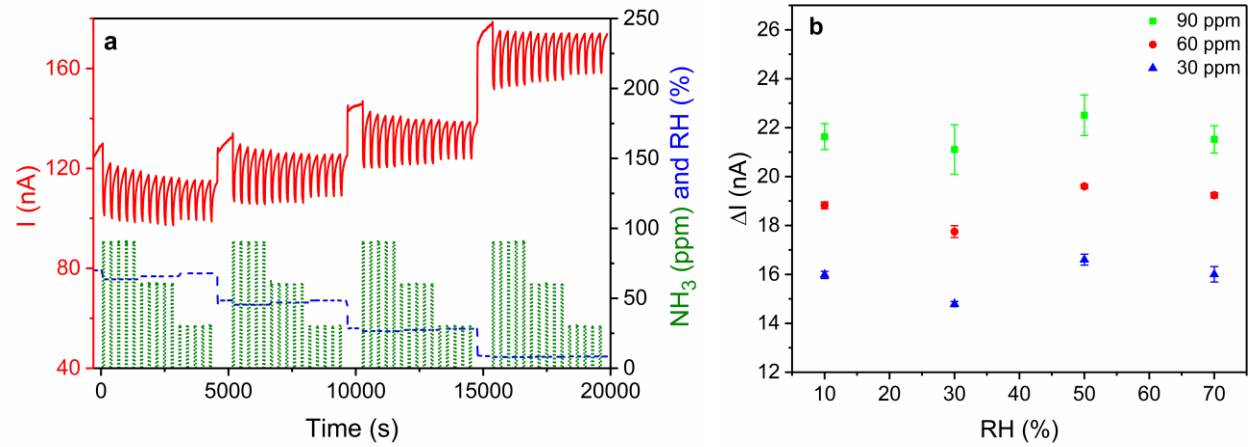

Figure 12. a) Current as a function of time of a PTFANI/$LuPc_2$ heterojunction exposed to NH_3 (90, 60 and 30 ppm), in humid air, from 70% RH to 10% RH, during exposure/recovery cycles (1 min / 4 min); b) ΔI response (mean value over cycles) at 90, 60 and 30 ppm of NH_3 concentration and at different RH values; the error bars represent the standard deviation.

In the literature, when the effect of the humidity is studied, the experiment is either carried out independently of NH_3, in a separate experiment, so the synergy between NH_3 and water is not taken into account,[66] or the response to NH_3 is studied in wet atmosphere, but only at a particular RH value and not in a broad range.[67] Thus, the response of a PANI resistor was studied in a broad range of RH, but only at 100 ppm NH_3, moreover with very long exposures (4 h).[68] Only few examples of ammonia sensors were reported with a response that does not depend on the RH value. We can cite one work based on PANI associated to a cobalt sulfonated phthalocyanine deposited by the layer-by-layer technique,[9] which is difficult to industrialize for mass production. The review of C. di Natale et al. on gas sensors for breath analysis[65] reports devices with a LOD lower than this obtained in the present study. However, in the first case, sulfuric acid is used as sensing liquid[69] that is not very friendly for a current use. In the second case, a sub-ppm LOD is also observed, but the sensor operates at 500 °C and the performance of the sensor is maintained only up to 25% RH.[70] Even though, we did not study the selectivity of the devices in the present

work, we know that the $LuPc_2$ cover layer brings a sensitivity to oxidizing and reducing species rather than to other volatile organic compounds. Indeed, due to its radical nature, $LuPc_2$ is easily oxidized and reduced. However, oxidizing analytes can be distinguished from donating analytes, since their responses will be opposite, as already shown with p-type and n-type phthalocyanine-based MSDI heterojunctions.[57] We would also mention that many applications of the ammonia detection deals with food industry where ammonia needs to be measured in building without strong oxidizing agent (with neither ozone nor nitrogen dioxide), but in humid atmospheres. So, the present device favorably competes with previously reported ammonia sensors, both for its rather low sensitivity to RH variations and for its sub-ppm LOD.

4. Conclusion

We achieved a comprehensive study of PTFANI over a large pH range, from -2 (H_0) to +7. The electrochemical oxidation of TFANI leads to a brown, poorly conductive polymer, the form of which varies with the pH and the applied potential.

For pH below 1.85, globally no proton transfer takes place during the electrochemical study, but the insertion of anions at the site of the protonated imines was investigated by both EQCM and XPS experiments. PTFANI shows a lower ratio of 1 ClO_4^- per 3 TFANI units compared to that of PANI (1 ClO_4^- / aromatic unit). This was confirmed by the oxidation degree of the emeraldine salt calculated by both XPS and UV-visible spectroscopy. In this region, the transition occurs between the leucoemeraldine base and the emeraldine salt forms. However, contrary to polyaniline, the polymer conductivity is not affected by the insertion of anions. This is certainly caused by the electron-withdrawing effect of the fluorinated substituents, which

makes the imine protonation more difficult. The formation of a structure with high electron delocalization plays a significant role in the increased conductivity of PANI.

The behavior at pH > 1.85 is different for PTFANI compared to PANI; there is no anion upload during the electron transfer (see EQCM results at pH 4), but one proton per electron is involved during the transition between the leucoemeraldine base and the emeraldine base forms. It should also be noted that the oxidation of the emeraldine to the pernigraniline form is not accessible in PTFANI.

Thanks to the low conductivity of PTFANI, we were able to build a heterojunction, by adding a top layer of the lutetium bisphthalocyanine as a highly conductive semiconductor. The double lateral heterojunction was used to detect ammonia, at room temperature, with a good stability of the response in a broad relative humidity range (10-70 %) and with a sub-ppm LOD.

Supporting information

Chronoamperograms of PTFANI and PANI; detailed reaction schemes for PANI and PTFANI; Cl(1s) and F(1s) XPS, IR, DSC, TGA, ^{1}H and ^{19}F NMR of PTFANI; and response of a PTFANI/$LuPc_2$/PTFANI heterojunction to NH_3 in the range 10-90 ppm (PDF**).**

Acknowledgments

The authors acknowledge the *Agence Nationale de la Recherche* for funding through the ANR projects CAP-BTX ANR-BLAN-2010-917-02 and OUTSMART ANR-2015-CE39-0004-03 and the MENESR for a PhD grant (M. M.). Financial support from the European Union (FEDER) and the *Conseil Régional de Bourgogne* through the FABER and the PARI SMT 08 and CDEA programs is gratefully acknowledged. We also acknowledge the *Conseil Régional de Bourgogne*

through the CPER program. We would like to thank the European Union for funding through the COST action TD1105 EuNetAir.

Corresponding Authors

* marcel.bouvet@u-bourgogne.fr; * rita.meunier-prest@u-bourgogne.fr

Author Contributions

The manuscript was written through contributions of all authors. All authors have given approval to the final version of the manuscript.

References

(1) MacDiarmid, A. "Synthetic Metals": a Novel Role for Organic Polymers (Nobel Lecture). *Angew. Chem. Int. Ed.* **2001**, *40* (14), 2581–2590.

(2) Peet, J.; Heeger, A. J.; Bazan, G. C. "Plastic" Solar Cells: Self-Assembly of Bulk Heterojunction Nanomaterials by Spontaneous Phase Separation. *Acc. Chem. Res.* **2009**, *42* (11), 1700–1708.

(3) Epstein, A. J.; MacDiarmid, A. G. Polyaniline Versus Polyacetylene, or, Rings Versus Bonds and the Roles of Barriers and Crystallinity. In *Conjugated Polymeric Materials: Opportunities in Electronics, Optoelectronics, and Molecular Electronics*; Brédas, J. L., Chance, R. R., Eds.; Springer Netherlands: Dordrecht, 1990; pp 195–205.

(4) Janata, J.; Josowicz, M. Conducting Polymers in Electronic Chemical Sensors. *Nat. Mater.* **2003**, *2* (1), 19–24.

(5) Hatchett, D. W.; Josowicz, M. Composites of Intrinsically Conducting Polymers as Sensing Nanomaterials. *Chem. Rev.* **2008**, *108* (2), 746–769.

(6) Hatfield, J. V.; Neaves, P.; Hicks, P. J.; Persaud, K.; Travers, P. Towards an Integrated Electronic Nose Using Conducting Polymer Sensors. *Sens. Actuators: B. Chem.* **1994**, *18* (1-3), 221–228.

(7) Nicolas-Debarnot, D.; Poncin-Epaillard, F. Polyaniline as a New Sensitive Layer for Gas Sensors. *Anal. Chim. Acta* **2003**, *475* (1-2), 1–15.

(8) Meijerink, M. G. H.; Strike, D. J.; de Rooij, N. F.; Koudelka-Hep, M. Reproducible Fabrication of an Array of Gas-Sensitive Chemo-Resistors with Commercially Available Polyaniline. *Sens. Actuators: B. Chem.* **2000**, *68* (1-3), 331–334.

(9) Gaudillat, P.; Jurin, F.; Lakard, B.; Buron, C.; Suisse, J.-M.; Bouvet, M. From the Solution Processing of Hydrophilic Molecules to Polymer-Phthalocyanine Hybrid Materials for Ammonia

Sensing in High Humidity Atmospheres. *Sensors* **2014**, *14* (8), 13476–13495.

(10) Mérian, T.; Redon, N.; Zujovic, Z.; Stanisavljev, D.; Wojkiewicz, J. L.; Gizdavic-Nikolaidis, M. Ultra Sensitive Ammonia Sensors Based on Microwave Synthesized Nanofibrillar Polyanilines. *Sens. Actuators: B. Chem.* **2014**, *203*, 626–634.

(11) Wan, P.; Wen, X.; Sun, C.; Chandran, B. K.; Zhang, H.; Sun, X.; Chen, X. Flexible Transparent Films Based on Nanocomposite Networks of Polyaniline and Carbon Nanotubes for High-Performance Gas Sensing. *Small* **2015**, *11* (40), 5409–5415.

(12) Domanský, K.; Baldwin, D. L.; Grate, J. W.; Hall, T. B.; Li, J.; Josowicz, M.; Janata, J. Development and Calibration of Field-Effect Transistor-Based Sensor Array for Measurement of Hydrogen and Ammonia Gas Mixtures in Humid Air. *Anal. Chem.* **1998**, *70* (3), 473–481.

(13) Timmer, B.; Olthuis, W.; Berg, A. V. D. Ammonia Sensors and Their Applications—a Review. *Sens. Actuators: B. Chem.* **2005**, *107* (2), 666–677.

(14) Zotti, G.; Comisso, N.; D'Aprano, G.; Leclerc, M. Electrochemical Deposition and Characterization of Poly(2,5-Dimethoxyaniline): a New Highly Conducting Polyaniline with Enhanced Solubility, Stability and Electrochromic Properties. *Adv. Mater.* **1992**, *4* (11), 749–752.

(15) D'Aprano, G.; Leclerc, M.; Zotti, G.; Schiavon, G. Synthesis and Characterization of Polyaniline Derivatives: Poly(2-Alkoxyanilines) and Poly(2,5-Dialkoxyanilines). *Chem. Mater.* **1995**, *7* (1), 33–42.

(16) Athawale, A. A.; Patil, S. F.; Deore, B.; Patil, R. C.; Vijayamohanan, K. Poly(M-Chloroaniline): Electrochemical Synthesis and Characterization. *Polym. J.* **1997**, *29* (10), 787–794.

(17) Díaz, F. R.; Sánchez, C. O.; del Valle, M. A.; Tagle, L. H.; Bernede, J. C.; Tregouet, Y. Synthesis, Characterization and Electrical Properties of Dihalogenated Polyanilines. *Synth. Met.* **1998**, *92* (2), 99–106.

(18) Cihaner, A.; Önal, A. M. Electrochemical Behaviour and Electrochemical Polymerization of Fluoro-Substituted Anilines. *Polym. Int.* **2002**, *51* (8), 680–686.

(19) Cassidy, J.; Breen, W. Electrochemical Formation of Fluorinated Polyaniline. *Synth. Met.* **1991**, *43* (1), 3059–3062.

(20) Astratine, L.; Magner, E.; Cassidy, J.; Betts, A. Characterization and Electrochromic Properties of Poly(2,3,5,6-Tetrafluoroaniline): Progress Towards a Transparent Conducting Polymer. *Electrochim. Acta* **2012**, *74*, 117–122.

(21) Kirin, I. S.; Moskalev, P. N.; Makashev, Y. A. Formation of Unusual Phthalocyanines of the Rare-Earth Elements. *Russ. J. Inorg. Chem.* **1965**, *10*, 1065–1066.

(22) Britton, H. T. S.; Robinson, R. A. CXCVIII.—Universal Buffer Solutions and the Dissociation Constant of Veronal. *J. Chem. Soc.* **1931**, *0* (0), 1456–1462.

(23) McGuire, G. E.; Schweitzer, G. K.; Carlson, T. A. Core Electron Binding Energies in Some Group IIIA, VB, and VIB Compounds. *Inorg. Chem.* **1973**, *12* (10), 2450–2453.

(24) Gaudillat, P.; Wannebroucq, A.; Suisse, J.-M.; Bouvet, M. Bias and Humidity Effects on the Ammonia Sensing of Perylene Derivative/Lutetium Bisphthalocyanine MSDI Heterojunctions. *Sens. Actuators: B. Chem.* **2016**, *222*, 910–917.

(25) Mareček, V.; Samec, Z.; Weber, J. The Dependence of the Electrochemical Charge-Transfer Coefficient on the Electrode Potential. *J. Electroanal. Chem.* **1978**, *94* (3), 169–185.

(26) Huang, W.-S.; Humphrey, B. D.; MacDiarmid, A. G. Polyaniline, a Novel Conducting Polymer. Morphology and Chemistry of Its Oxidation and Reduction in Aqueous Electrolytes. *J. Chem. Soc., Faraday Trans. 1* **1986**, *82* (8), 2385–2400.

(27) Focke, W. W.; Wnek, G. E.; Wei, Y. Influence of Oxidation State, pH, and Counterion on the Conductivity of Polyaniline. *J.Phys. Chem.* **1987**, *91* (22), 5813–5818.

(28) Laviron, E. Electrochemical Reactions with Protonations at Equilibrium. Part VIII. the 2 e^-, 2 H^+ Reaction (9-Member Square Scheme) for a Surface or for a Heterogeneous Reaction in the Absence of Disproportionation and Dimerization Reactions. *J. Electroanal. Chem.* **1983**, *146* (1), 15–36.

(29) Meunier-Prest, R.; Laviron, E. Electrochemical Reactions with Protonations at Equilibrium. Part XV. the $2e^-$, $2h^+$ Bi-Cubic Scheme. *J. Electroanal. Chem.* **1992**, *328* (1-2), 33–46.
(30) Geniès, E. M.; Lapkowski, M. Spectroelectrochemical Study of Polyaniline Versus Potential in the Equilibrium State. *J. Electroanal. Chem.* **1987**, *220* (1), 67–82.
(31) Cushman, R. J.; McManus, P. M.; Cheng Yang, S. Spectroelectrochemical Study of Polyaniline: the Construction of a pH-Potential Phase Diagram. *J. Electroanal. Chem.* **1987**, *219* (1-2), 335–346.
(32) Huang, W.-S.; MacDiarmid, A. G.; Epstein, A. J. Polyaniline: Non-Oxidative Doping of the Emeraldine Base Form to the Metallic Regime. *J. Chem. Soc., Chem. Comm.* **1987**, No. 23, 1784–1786.
(33) Paul, M. A.; Long, F. A. H0 and Related Indicator Acidity Function. *Chem. Rev.* **1957**, *57* (1), 1–45.
(34) Daikhin, L. I.; Levi, M. D. Isotherms of Protonation and Titration Curves of Leucoemeraldine and Emeraldine. *Synth. Met.* **1992**, *52* (3), 367–376.
(35) Geniès, E. M.; Vieil, E. Theoretical Charge and Conductivity "State - Diagrams" for Polyaniline Versus Potential and pH. *Synth. Met.* **1987**, *20* (1), 97–108.
(36) Marmisollé, W. A.; Florit, M. I.; Posadas, D. Coupling Between Proton Binding and Redox Potential in Electrochemically Active Macromolecules. the Example of Polyaniline. *J. Electroanal. Chem.* **2013**, *707*, 43–51.
(37) Marmisollé, W. A.; Florit, M. I.; Posadas, D. Acid–Base Equilibrium in Conducting Polymers. the Case of Reduced Polyaniline. *J. Electroanal. Chem.* **2014**, *734*, 10–17.
(38) Hansch, C.; Leo, A.; Taft, R. W. A Survey of Hammett Substituent Constants and Resonance and Field Parameters. *Chem. Rev.* **1991**, *91* (2), 165–195.
(39) Gruger, A.; Novak, A.; Régis, A.; Colomban, P. Infrared and Raman Study of Polyaniline Part II: Influence of Ortho Substituents on Hydrogen Bonding and UV/Vis—Near-IR Electron Charge Transfer. *J.Mol. Struct.* **1994**, *328*, 153–167.
(40) Sharma, A. L.; Saxena, V.; Annapoorni, S.; Malhotra, B. D. Synthesis and Characterization of a Copolymer: Poly(Aniline-Co-Fluoroaniline). *J. Appl. Polym. Sci.* **2001**, *81* (6), 1460–1466.
(41) Han, C.-C.; Chen, H.-Y. Highly Conductive and Electroactive Fluorine-Functionalized Polyanilines. *Macromol.* **2007**, *40* (25), 8969–8973.
(42) Masters, J. G.; Sun, Y.; MacDiarmid, A. G.; Epstein, A. J. Polyaniline: Allowed Oxidation States. *Synth. Met.* **1991**, *41* (1-2), 715–718.
(43) Huang, W. S.; MacDiarmid, A. G. Optical Properties of Polyaniline. *Polymer* **1993**, *34* (9), 1833–1845.
(44) Mungkalodom, P.; Paradee, N.; Sirivat, A.; Hormnirun, P. Synthesis of Poly (2,5-Dimethoxyaniline) and Electrochromic Properties. *Mater. Res.* **2015**, *18* (4), 669–676.
(45) Cihaner, A.; Önal, A. M. Synthesis and Characterization of Fluorine-Substituted Polyanilines. *Eur. Polym. J.* **2001**, *37* (9), 1767–1772.
(46) Vijayanand, P. S.; Vivekanandan, J.; Mahudeswaran, A.; Jayaprakasam, R. Synthesis and Characterization of Aniline and 4-Fluoroaniline Conducting Copolymer Composites Doped with Silver Nanoparticles. *Macromol. Symp.* **2016**, *362* (1), 65–72.
(47) Wang, X.; Sun, T.; Wang, C.; Wang, C.; Zhang, W.; Wei, Y. 1H NMR Determination of the Doping Level of Doped Polyaniline. *Macromol. Chem. Phys.* **2010**, *211* (16), 1814–1819.
(48) Venancio, E. C.; Costa, C. A. R.; Machado, S. A. S.; Motheo, A. J. AFM Study of the Initial Stages of Polyaniline Growth on ITO Electrode. *Electrochem. Comm.* **2001**, *3* (5), 229–233.
(49) Lee, Y.-S. Syntheses and Properties of Fluorinated Carbon Materials. *J. Fluor. Chem.* **2007**, *128* (4), 392–403.
(50) Lipińska, M. E.; Rebelo, S. L. H.; Pereira, M. F. R.; Gomes, J. A. N. F.; Freire, C.; Figueiredo, J. L. New Insights Into the Functionalization of Multi-Walled Carbon Nanotubes with Aniline Derivatives. *Carbon* **2012**, *50* (9), 3280–3294.
(51) Kumar, S. N.; Gaillard, F.; Bouyssoux, G.; Sartre, A. High-Resolution XPS Studies of

Electrochemically Synthesized Conducting Polyaniline Films. *Synth. Met.* **1990**, *36* (1), 111–127.

(52) Park, O.-K.; Chae, H.-S.; Park, G. Y.; You, N.-H.; Lee, S.; Bang, Y. H.; Hui, D.; Ku, B.-C.; Lee, J. H. Effects of Functional Group of Carbon Nanotubes on Mechanical Properties of Carbon Fibers. *Compos. Part B: Eng.* **2015**, *76*, 159–166.

(53) Neoh, K. G.; Kang, E. T.; Tan, K. L. Thermal Degradation Studies of Perchlorate-Doped Conductive Polymers. *J. Appl. Polym. Sci.* **1991**, *43* (3), 573–579.

(54) Amin, M. A. Metastable and Stable Pitting Events on Al Induced by Chlorate and Perchlorate Anions—Polarization, XPS and SEM Studies. *Electrochim. Acta* **2009**, *54* (6), 1857–1863.

(55) Sizun, T.; Patois, T.; Bouvet, M.; Lakard, B. Microstructured Electrodeposited Polypyrrole–Phthalocyanine Hybrid Material, From Morphology to Ammonia Sensing. *J. Mater. Chem.* **2012**, *22* (48), 25246–25248.

(56) Park, S.; Park, C.; Yoon, H. Chemo-Electrical Gas Sensors Based on Conducting Polymer Hybrids. *Polymers* **2017**, *9* (5), 155.

(57) Parra, V.; Brunet, J.; Pauly, A.; Bouvet, M. Molecular Semiconductor-Doped Insulator (MSDI) Heterojunctions: an Alternative Transducer for Gas Chemosensing. *Analyst* **2009**, *134* (9), 1776–1778.

(58) Turek, P.; Petit, P.; Andre, J. J.; Simon, J.; Even, R.; Boudjema, B.; Guillaud, G.; Maitrot, M. A New Series of Molecular Semiconductors: Phthalocyanine Radicals. *J. Am. Chem. Soc.* **1987**, *109* (17), 5119–5122.

(59) Wannebroucq, A.; Gruntz, G.; Suisse, J.-M.; Nicolas, Y.; Meunier-Prest, R.; Mateos, M.; Toupance, T.; Bouvet, M. New n-Type Molecular Semiconductor–Doped Insulator (MSDI) Heterojunctions Combining a Triphenodioxazine (TPDO) and the Lutetium Bisphthalocyanine (LuPc2) for Ammonia Sensing. *Sens. Actuators: B. Chem.* **2017**.

(60) Bouvet, M.; Gaudillat, P.; Kumar, A.; Sauerwald, T.; Schüler, M.; Schütze, A.; Suisse, J.-M. Revisiting the Electronic Properties of Molecular Semiconductor – Doped Insulator (MSDI) Heterojunctions Through Impedance and Chemosensing Studies. *Org. Electron.* **2015**, *26*, 345–354.

(61) Murdey, R.; Sato, N.; Bouvet, M. Frontier Electronic Structures in Fluorinated Copper Phthalocyanine Thin Films Studied Using Ultraviolet and Inverse Photoemission Spectroscopies. *Mol. Cryst. Liq. Cryst.* **2006**, *455* (1), 211–218.

(62) Sakamoto, Y.; Suzuki, T.; Kobayashi, M.; Gao, Y.; Fukai, Y.; Inoue, Y.; Sato, F.; Tokito, S. Perfluoropentacene: High-Performance p−n Junctions and Complementary Circuits with Pentacene. *J. Am. Chem. Soc.* **2004**, *126* (26), 8138–8140.

(63) Facchetti, A.; Deng, Y.; Wang, A.; Koide, Y.; Sirringhaus, H.; Marks, T. J.; Friend, R. H. Tuning the Semiconducting Properties of Sexithiophene by α,ω-Substitution— α,ω-Diperfluorohexylsexithiophene: the First n-Type Sexithiophene for Thin-Film Transistors. *Angew. Chem.* **2000**, *112* (24), 4721–4725.

(64) *Directive 2008/50/EC of the European Parliament and of the Council of 21May 2008, on Ambient Air Quality and Cleaner Air for Europe*; 2008; Vol. L 152, pp 1–44.

(65) Di Natale, C.; Paolesse, R.; Martinelli, E.; Capuano, R. Solid-State Gas Sensors for Breath Analysis: a Review. *Anal. Chim. Acta* **2014**, *824*, 1–17.

(66) Benten, H.; Kudo, N.; Ohkita, H.; Ito, S. Layer-by-Layer Deposition Films of Copper Phthalocyanine Derivative; Their Photoelectrochemical Properties and Application to Solution-Processed Thin-Film Organic Solar Cells. *Thin Solid Films* **2009**, *517* (6), 2016–2022.

(67) Hirata, M.; Sun, L. Characteristics of an Organic Semiconductor Polyaniline Film as a Sensor for NH3 Gas. *Sens. Actuators A: Phys.* **1994**, *40* (2), 159–163.

(68) Matsuguchi, M.; Okamoto, A.; Sakai, Y. Effect of Humidity on NH3 Gas Sensitivity of Polyaniline Blend Films. *Sens. Actuators: B. Chem.* **2003**, *94* (1), 46–52.

(69) Toda, K.; Li, J.; Dasgupta, P. K. Measurement of Ammonia in Human Breath with a Liquid-Film Conductivity Sensor. *Anal. Chem.* **2006**, *78* (20), 7284–7291.

(70) Gouma, P.; Kalyanasundaram, K.; Yun, X.; Stanacevic, M.; Wang, L. Nanosensor and Breath Analyzer for Ammonia Detection in Exhaled Human Breath. *IEEE Sensors J.* **2010**, *10* (1), 49–53.

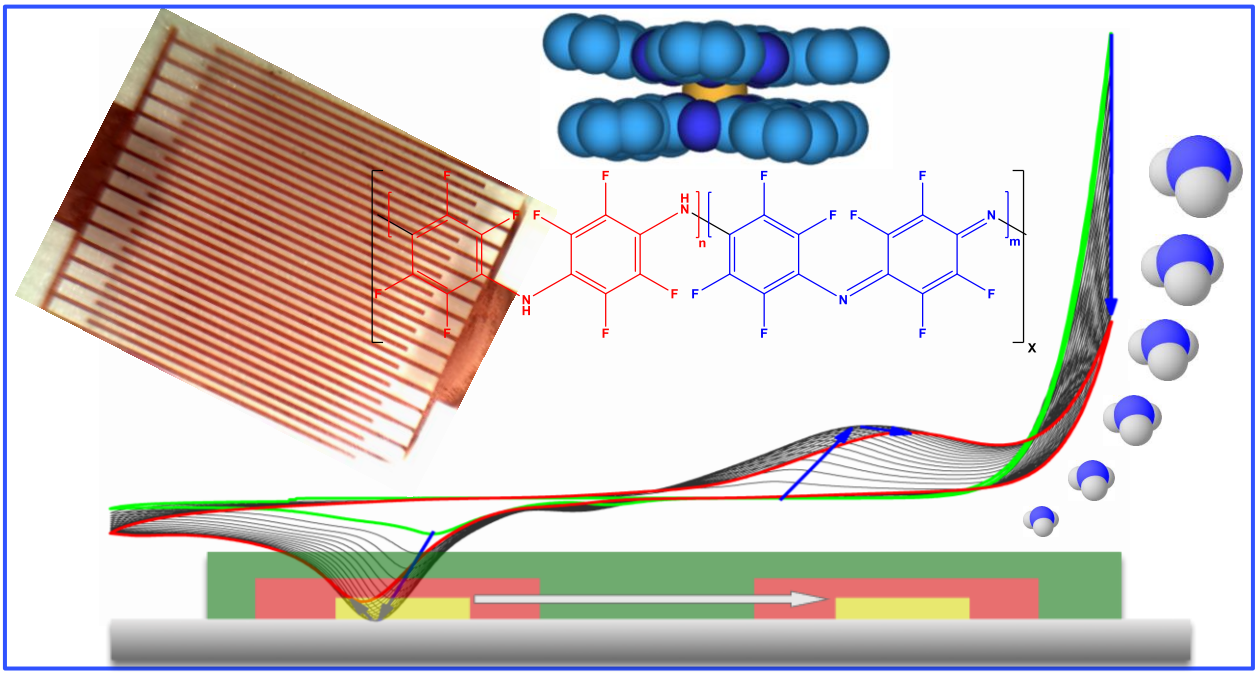

Graphical abstract